ORIGINAL PAPER

Higher Himalaya in the Bhagirathi section (NW Himalaya, India): its structures, backthrusts and extrusion mechanism by both channel flow and critical taper mechanisms
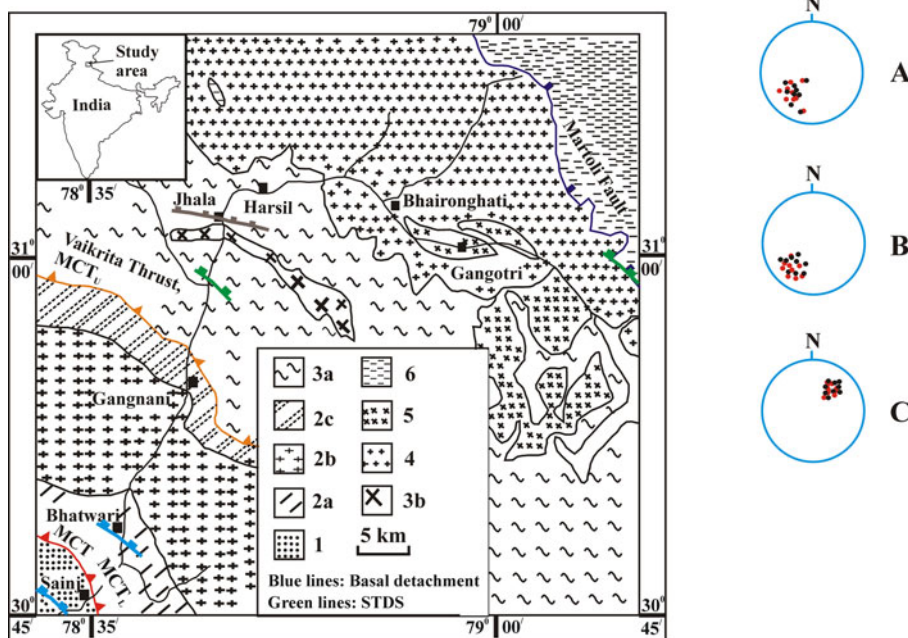
Soumyajit Mukherjee

Abstract The Higher Himalayan Crystalline (HHC) in the Bhagirathi river section (India) on fieldwork reveals two extensional ductile top-to-N/NE shear sub-zones—the 'South Tibetan Detachment System' and the 'Basal Detachment'—besides a preceding top-to-S/SW ductile shear. A top-to-N/NE brittle shear was identified as backthrusts from the HHC (except its northern portion) that occur repeatedly adjacent to numerous top-to-S/SW brittle shears as fore-thrusts. The northern portion of the HHC—the Gangotri Granite—exhibits infrequent total six extensional and compressional brittle shear senses. The backthrusts could be due to a low friction between the lower boundary of the HHC (i.e. the Main Central Thrust-Zone) and the partially molten hot rock materials of the HHC. Subduction of the Eurasian plate towards S/SW below the Indian plate more extensively in the Garhwal sector could be the second possible reason. Presence of two ductile extensional shear sub-zones may indicate channel flow (or several exhumation mechanisms) of the HHC in a shifting mode (similar to Mukherjee et al. in Int J Earth Sci 101:253–272, 2012). The top-to-S/SW extensional brittle shear exclusively within the upper (northern portion) of the HHC and a top-to-S/SW brittle shear within the remainder of it is a possible indicator of critical taper deformation mechanism. Thus, this work provides the field evidences of possibly both channel flow and critical taper conditions from a Higher Himalayan section, besides that by Larson et al. (Geol Soc Am Bull 122:1116–1134, 2010).

S. Mukherjee (✉)
Department of Earth Sciences, Indian Institute of Technology Bombay, Powai, Mumbai 400076, Maharashtra, India
e-mail: soumyajitm@gmail.com

Introduction

How deep metamorphic rocks extrude is important to interpret the progressive deformation history of the convergent orogens. By sequential foreland propagating thrusting, these orogens accommodate crustal shortening of around a few 100 km (Panian and Pilant 1990). Newer thrusts of same dip direction develop towards the foreland and extrude rock masses towards the later at non-uniform intervals of several million years (Yin 2006). At least four additional regional structures/deformations may complicate this simple scenario viz. (1) foreland verging out-of-sequence thrusts that activate inside the previously thrust-up rock mass; (2) hinterland verging back thrusting; and (3) backslip of the interface between the two plates (Butler 1987; Morley 1988; Wang 2007; Larson et al. 2010; Catlos et al. 2007; Mukherjee et al. 2012 but many others). Additionally, around the late phase of collision for the large hot orogens, low-viscosity partially molten material may extrude in a single- or multiple pulses through one of the 'shear zones' ('channels') (e.g. Beaumont et al. 2001; Brown and Gibson 2006; Hollister and Grujic 2006; Rivers 2009; Mukherjee 2012a; Mukherjee and Koyi 2010a, b; Mukherjee et al. 2012), along with intermittent critical taper mechanism (Chambers et al. 2011; Larson et al. 2011) leading to a significant viscous dissipation (Mukherjee 2012a). Alternately, critical taper mechanism drove the channel flow (Long et al. 2012). Thermobarometric studies from central Bhutan Himalaya led Corrie et al. (2012)

A: Poles of C-shear planes for top-to-SW compressional (orange dots) & top-to-NE extensional shear (black dots) - inside the 'basal detachment'

B: Poles of C-shear planes for top-to-SW compressional (orange dots) & top-to-NE extensional shear (black dots) - inside the 'STDS' from south up to Harsil

C: Poles of Y-shear planes for top-to-NE compressional shear (backthrusting): black dots- inside 'basal detachment' orange dots- northward from Bhatwari

Fig. 1 The Higher Himalayan Crystalline (HHC) (from the MCT_L up to the Martoli Fault). *1* Lesser Himalayan sedimentary rocks; *2a* granite gneiss, mica schist; *2b* mylonitized augen gneiss, mica schist; *2c* phyllonite, chlorite schist; *3a* sill/ky/gt/bt/mus schist/gneiss, migmatite; *3b* augen Gneiss; *4* Bhaironghati Biotite Gneiss; *5* Gangotri Granite; *6* Tethyan Himalaya; MCT_L Main Central Thrust-Lower. Reproduced from Jain et al. (2002). In this work, *blue lines* demarcate the South Tibetan Detachment System (STDS) and *green lines* the "basal detachment". MCT_U Main Central Thrust-Upper. The Jhala Normal Fault is traced as per fig. 2 of Catlos et al. (2002)

to propose that the Higher Himalaya underwent an 'orogenic flattening', which is a combination of a stronger critical taper and a weaker channel flow mechanism. Notice that neither channel flow (reviewed in Appendix-1 in Mukherjee 2012b, c) nor critical taper alone (as mentioned in Johnson and Harley 2012) can explain all the tectonic constrains of the Higher Himalaya.

Given its structural and metamorphic characters, the Higher Himalaya (Fig. 1)—one of the intra-continental longitudinal tectonic units of the Himalayan arc—has gained paramount attention for its exhumation mechanism (latest review by Mukherjee 2012b). Note that a zone bound by two shear zones can also lead to exhumation of high pressure rocks (e.g. Malavieille et al. 1998; Mukherjee and Mulchrone 2012). This work presents field-based

structural geology of the Higher Himalaya Crystalline (HHC) from the Bhagirathi river section, NW Himalaya, India. Based mainly on the new findings of two ductile extensional sheared sub-zones and the brittle shear senses, the major deformation phases of the HHC is speculated. The shear sense indicators are usually of decimetre scale, whereas the identified brittle faults can be traced in near vertical sections.

Geology and tectonics

The Precambrian and Proterozoic HHC rocks along with Ordovician orthogneiss and Miocene leucogranites are dominantly gneisses and schists metamorphosed to

greenschist to amphibolite facies (Yin 2006) and consist of patches of granulites and metabasites (Zhang et al. 2010's review). The HHC could either be differently metamorphosed equivalents of the underlying Lesser- and the overlying Tethyan Himalayan units, or is a mélange of several crustal units with the Greater India during an early Paleozoic tectonics, that subsequently underwent extrusion by channel flow initiating from the mid-crustal rocks of south Tibet and/ or by wedge mechanism (review: Gehrels et al. 2011).

The HHC is bound by the MCT-zone at the bottom at south and the South Tibetan Detachment System (STDS) as the top at north (Fig. 1). The upper (i.e. the northern) portion of the HHC migmatized due to extrusion of voluminous granitic melt coeval to the ductile extensional shear within the STDS. Throughout the HHC, a top-to-S/SW ductile shear from ~25 Ma took place. Limited geochronologic data indicate that the interior of the HHC was sheared between ~25–18 Ma (Carosi et al. 2013; Iaccarino et al. 2013). The 25 Ma timing nearly the same as that for the 'hard collision' between the Indian lithosphere and the Eurasian plate (van Hinsbergen et al. 2012). A late-phase ductile extensional shear within 19–14 Ma has been documented from the STDS (review by Godin et al. 2006). Inside the HHC, a ductile extensional shear during 24–12 Ma has also been reported from the 'South Tibetan Detachment System-Lower' inside the HHC, which is present rather discontinuously along the

Himalayan trend (e.g. Carosi et al. 1998; Law et al. 2004; review by Godin et al. 2006). To avoid confusion with the original usage of the term 'South Tibetan Detachment', the extensional shear zone at the bottom of the HHC henceforth is described as the 'basal detachment'. The part of the HHC not included inside the STDS and the basal detachment is top-to-S/SW sheared and may not be undeformed. Also regionally discontinuous is the geochronologically established out-of-sequence thrust plane inside the HHC active from 22 Ma till the Holocone, which is devoid of any unique structures across it (review by Mukherjee et al. 2012). The HHC, especially the Sutlej river in Himachal Pradesh (India), has revealed inverted metamorphism (Vannay et al. 2004). The MCT-zone has also revealed inverted metamorphism (from Nepal: Lombardo et al. 1993; Goscombe et al. 2006). Metamorphism within the HHC was either during the Eo-Himalayan (>44–33 Ma) and the Neo-Himalayan (~mid-Miocene) periods (reviewed as fig. 7a in Streule et al. 2010) or as a single phase (review by Yakymchuk and Godin 2012). A regional kyanite to sillimanite-grade metamorphism during 32-20 Ma took place within the HHC (St-Onge et al. 2006). The HHC could have undergone a HP metamorphism at a depth of ~80–100 km (Yang et al. 2011), but not many supports this.

The HHC in the Bhagirathi section in particular consists of garnet-biotite schists and gneisses, metadolerites,
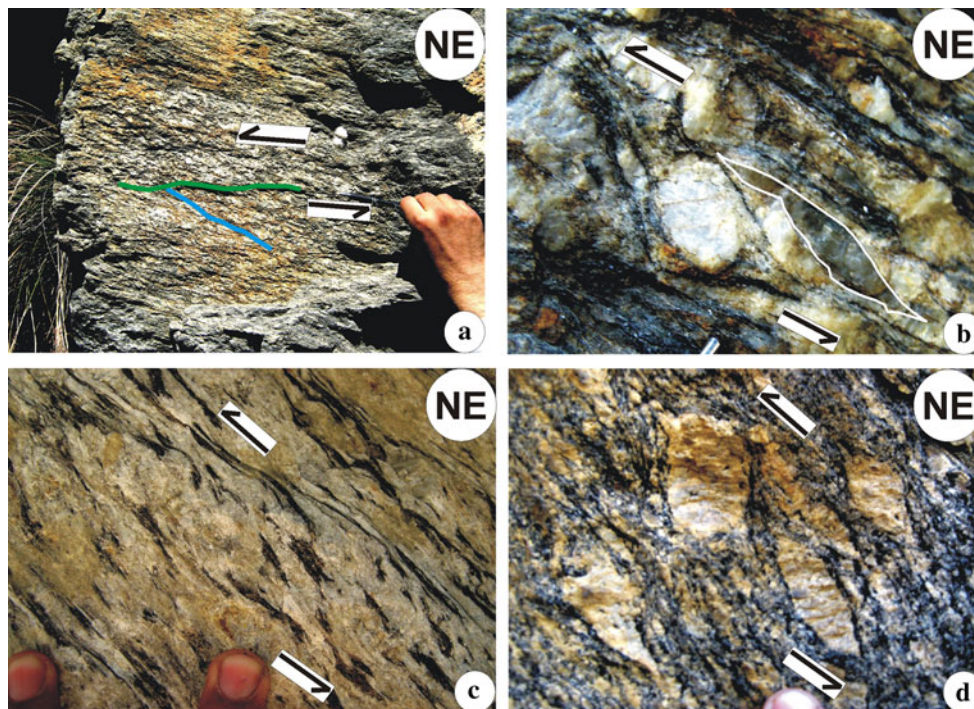

Fig. 2 Top-to-SW ductile shear sense indicators from the HHC, Bhagirathi section. a Mylonite with sub-horizontal C-planes. Location-2; at Sainj (30°45′19.4″N; 78°34′31.4″E). b A delta structure. Adjacent to it is a sigmoid elongated quartz Location-4. (30°48′1.8″N; 78°37′00″E). c Top-to-SW ductile shear sense indicators from the HHC, Bhagirathi section. S-C fabric defined by biotites. Location— 30°51′37″N; 78°39′2.6″E. d Sigmoid and lenticular feldspar clasts. Width of photo: 18 cm. Location-6 30°0′42″N; 78°42′25.6″E

phyllonites, actinolite schists, carbonates, calc-silicates, talc-tremolite schist, amphibolites, migmatites and granites (Metcalfe 1993; Singh and Thakur 2001; Srivastava and Tripathi 2007; Jain et al. 2002; Tripathi et al. 2009; Sachan et al. 2010). The Bhagirathi Granite (/Badrinath Granite/ Gangotri Granite)—located at the northern portion of the HHC—has been described as en-echelon lensoid intrusions consisting of potassium feldspar, quartz, plagioclase, tourmaline, muscovite, biotite and garnet (Searle et al. 1993) that might had formed from a Pan-African rock body (Singh et al. 2003). This granite body exhumed at a much faster rate initiating from ∼2.4 Ma with a concomitant denudation at a rate of ∼2 mm year^{-1} (Sorkhabi et al. 1996). For a much broader span during 21–5 Ma, the middle of the HHC in the Garhwal Himalaya exhumed at a rate of ∼0.67 ± 0.13 mm year^{-1} (Yin 2006). Linero (2008) deduced a near constant exhumation rate of the HHC in the Bhagirathi section of 1.43 mm year^{-1} since last ∼20 Ma. Scaillet et al. (1995) surmised that the granite body was emplaced during extensional shear of the upper boundary of the HHC (also see Searle et al. 1993). Jain et al. (2002), from a review of previous geochronologic data available from the Bhagirathi Granite, considered 22–23 Ma as its most plausible cooling age and 3 mm year^{-1} its exhumation rate. The cooling rate of the Higher Himalayan granite in the Garhwal Himalaya drastically reduced from ∼175–300 up to ∼16–20 °C km^{-1} from 23-01 Ma (Searle et al. 1999).

Around 10 km thick MCT-zone bound by the MCT (=MCT$_L$ of Godin et al. 2006 = Munsiari Thrust as referred in Catlos et al. 2002 = MCT$_2$ as followed by Mitra et al. 2010) at south, and the Vaikrita Thrust (=MCT$_U$ of Godin et al. 2006 = MCT$_1$ as followed by Mitra et al. 2010; also see Khannal and Robinson 2012) at north in the Garhwal Himalaya has been studied in greater detail than its further northern portions in the Bhagirathi section. Based on ^{40}Ar/^{39}Ar plateau age of hornblende, Metcalfe (1993) deduced that the MCT in the Garhwal sector was active at ∼19.8 ± 2.6 Ma. This broadly matches with the relatively brief span of 21–19 Ma of activation of the MCT-zone in this portion of the Himalaya (Searle et al. 1999). Catlos et al. (2002) obtained a much younger monazite age of 5.9 ± 0.2 Ma from the MCT$_U$. The MCT-zone shows an increasing grade of metamorphism towards N starting from chlorite up to the kyanite grade. An increase in temperature from 500 to 770 °C was also deciphered in structural up-section across this zone (Metcalfe 1993). Extrusion took place from north to south under decreasing thermobarometric conditions (Sachan et al. 2001). Near the MCT, mylonitized quartzite, S-C fabrics, prominent stretching lineations of micas and feldspars, and recrystallization of grains were reported (Singh and Thakur 2001; Jain et al. 2002; Tripathi et al. 2009). Three phases of folding were

documented from the entire HHC (Jain et al. 2002), and specifically from the MCT-zone (Srivastava and Tripathi 2007; Tripathi et al. 2009; also see Roy and Valdiya 1988)—but none of these deformations seem to be regional. This is supported by a near uniform N/NE dip of the 'main foliations' (or the primary shear C-planes of Passchier and Trouw 2005; e.g. Jain et al. 2002). A heterogeneous deformation led to ≥140–210 km displacement within the MCT-zone in the Garhwal region (Singh and Thakur 2001; Tripathi et al. 2009). Singh and Thakur (2001) deduced a strain ratio of 2.3:1.8:1 from the MCT-zone. Further, Tripathi and Srivastava (2005) deciphered shearing in conjugate sets, and a NNE–SSW compression simultaneous to the slip of the MCT (also see Srivastava et al. 2000). The middle of the MCT-zone underwent maximum strain and the magnitude fell down away from there in response to a non-coaxial shear (Srivastava et al. 2000; also see Grasemann et al. 1999 for another section). The MCT has been considered by some as a 'defunct Miocene structure' (Kirby and Whipple 2012). Although the component of pure shear has been deduced from a number of sections of the HHC (reviewed in fig. 8 of Mukherjee 2012b; also see Larson and Godin 2009), a similar quantification has not been done along the entire length of the Bhagirathi river within the HHC.

Mukherjee and Koyi (2010a) demarcated the STDS as a top-to-N/NE ductile extensional shear zone at the Sutlej section. The northern boundary of the STDS matched with the contact between the Higher and the Tethyan Himalaya and the southern boundary falls between the locations Pangi and Kashang. In contrary, the tectonics of the Bhagirathi section of the HHC is not yet well understood since the southern boundary of the STDS remained unmarked. Yin (2006) interpreted Metcalfe's (1993) data of uniform cooling age of ∼21 Ma across the Jhala fault inside the HHC as indicative of its inactivation during the Miocene Period of coeval compressional shear within the MCT and extensional shear of the STDS. In contrast to Sorkhabi et al.'s (1999) interpretation that it is purely a thrust, Catlos et al. (2002) and Yin (2006) considered that the Jhala Fault underwent a normal sense of movement in its late stage. Does the Jhala Fault demarcate the southern boundary of the STDS?

Structural geology

Ductile deformations

The HHC is top-to-S/SW ductile sheared. The primary shear C-planes dip towards N/NE. The spacing between the C-planes varies from ∼1 to 15 cm. The shear is exemplified by S-C fabrics and usually sigmoid-shaped clasts (Berthé et al. 1979; Mukherjee and Bandyopadhyay 2011;

Mukherjee 2011) of various morphologies (Figs. 2, 3). Some of the S-planes are defined by sigmoid quatzofeldspathic grains akin to sigma-structures (Fig. 2d), very rare delta (δ) structures (Fig. 2b), isolated curved grains of biotites (Fig. 2c), lenticular feldspar clasts with major axes tilted along the shear direction (Fig. 2d) etc. Delta structures indicate possibly a higher rate of rotation than the sigma (σ) structures (Passchier and Trouw 2005). Therefore, rare occurrence of the former structures indicates qualitatively a variation in the intensity of shear within the HHC. Also, different shapes of shear sense indicators occur side by side, such as the delta structures and individual grains of sigmoid shapes (Fig. 2d). At a few locations, the C-planes are sub-horizontal (Fig. 2a).

A top-to-N/NE extensional ductile shear confines within two sub-zones. The same set of N/NE dipping main foliations bound the S-fabrics. The extensional zone in south, demarcated by blue lines in Fig. 1, covers partly the MCT-zone and is designated as the 'basal detachment'. Its upper boundary is close to the village Bhatwari and is ∼20 km SW from the Vaikrita Thrust (=MCT$_U$). Strongly asymmetric quartzofeldspathic grains of various thicknesses define this shear (Fig. 3a, b). Close-spaced (cm to mm scale) C-planes and at places S-fabrics sub-parallel to the C-planes connote intense shear (interpreted as per Davis and Reynolds 1996; Twiss and Moores 2007). These extensional sub-zones were deciphered based on structures and fabrics, usually of cm scale, on rocks that can be closely observed exposed on the metal road section. For rocks exposed far away and across the road, it was not possible to trace the shear fabrics. Thus, the observed boundaries of those two extensional sub-zones were located only on the road/river section. For the sake of presentation, those have been drawn as short lines. In reality, those moderately dip towards NE.

The green lines in Fig. 1 demarcate the 'South Tibetan Detachment System-Upper' (STDS) as the second extensional zone. It occurs near the northern/upper portion of the HHC. The shear senses are indicated mainly by sigma-like structures of asymmetric quartzofeldspathic aggregates and veins (Fig. 4a–c) and one rare delta-like structure (Fig. 4d). The upper boundary of the STDS is the Malari Fault. The southern boundary lies ∼5 km SW to the location Jhala. Thus, the 'Jhala Normal Fault' is a part of the STDS and lies inside the latter. This is as per Searle et al.'s (1999) postulation but does not match with Catlos et al. (2002) who demarcated the Jhala Fault as the northern boundary of the Higher Himalaya by excluding the Gangotri Granite from the latter. Notice that except the upper boundary of the STDS, none of the other three boundaries of these two extensional zones coincide with any litho-contacts. This matches with the HHC in the Everest massif, Nepal Himalaya (Searle 1999) and Gonto La in southern Tibet (Edwards et al. 1996). In these locations, the basal detachment occurs much NE to the MCT$_L$. However, it mismatches with the Sutlej section of the HHC where Mukherjee and Koyi (2010a) demarcated the basal detachment nearly coincident with the MCT$_U$. Within the STDS and the basal detachment, fabrics of top-to-S/SW shear are less frequent than the top-to-N/NE ones. Therefore, following the standard explanation (Patel et al. 1993; Argles and Edwards 2002; Yin 2006; Mukherjee and Koyi 2010a, b), the S/SW shear might have preceded the N/NE one. Notice that an extensional ductile shear zone in the lower portion of the HHC in Nepal has also been referred by Sapkota and Sanislav (2012).

No clear-cut secondary shear planes—C' and C'' (Passchier and Trouw 2005) associate with the primary shear S-C fabrics for the top-to-S/SW and the top-to-N/NE shear. This possibly indicates insignificant pure shear component associated with that primary shear (interpretation as per Goscombe et al. 2006). Localized shear zones at low angles to the main foliation, however, occur exclusively within the pinch and swell structures (Fig. 5). Therefore, these might be due to local coaxial deformation that gave rise to boudins and do not have any tectonic implications (as per Schmalholz and Maeder 2012). Pinch and swell structures indicate non-Newtonian rheology of the matrix (Schmalholz and
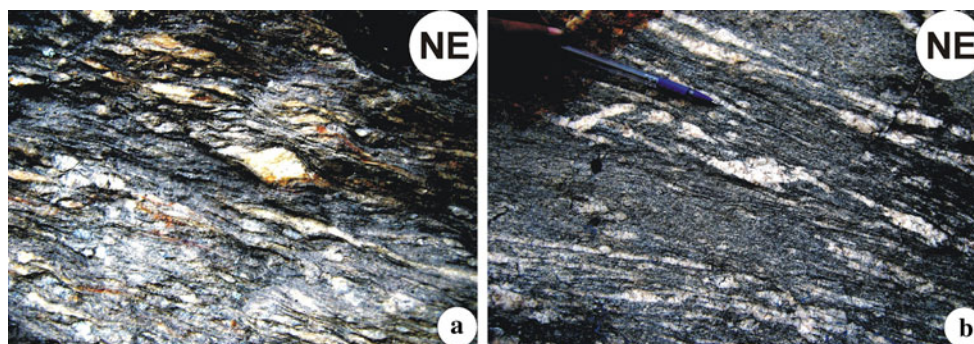

Fig. 3 a, b Extensional top-to-NE ductile shear inside the basal detachment—from sigmoidal quartzofeldspathic mineral aggregates within mylonitized gneiss. a Width of photo: 14 cm. Location: Near the MCT$_L$, Sainj village (30°46'14.2"N; 78°35'51.8"E)
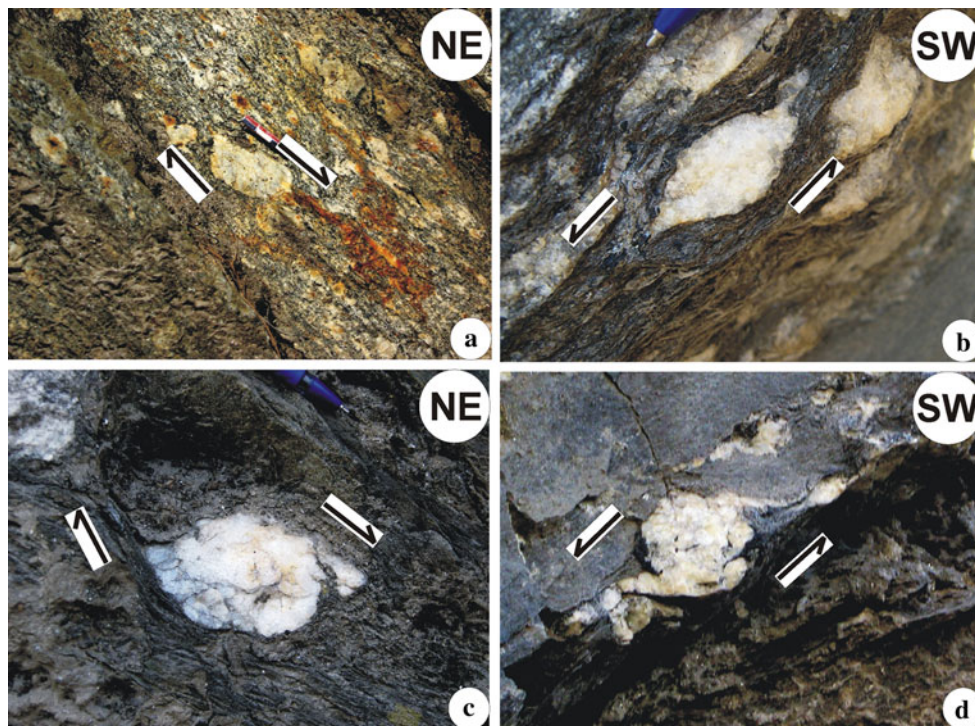
Fig. 4 Top-to-NE sense of ductile shear within the STDS (near the *upper portion* of the HHC). **a**, **b**, **d** Sigma-like structure of quartz vein; photo widths: ∼17 cm; **c** a delta-like structure. Photo width: ∼40 cm.

Locations: **a** 31°0′53.1′N, 78°42′29.4′E; **b** 31°01′56.6″N; 78°43′15.2″E; **c** 31°02′5.9″N; 78°43′31.8″E; **d** 31°01′18″N; 78°52′16.7″E

Maeder 2012). Therefore, modelling the HHC as a non-Newtonian fluid to explain its extrusion (Beaumont et al. 2001) is more appropriate than those based on its Newtonian rheology (such as Mukherjee 2012d). The geometry of scar folds varies considerably in these boudins. Where the matrix is non-foliated, these folds obviously did not develop. Variation in geometry of these folds could be explained by either a disparity in the intensity of shear or due to different viscosity contrasts between the clasts and the matrices (Maeder et al. 2009).

Brittle deformations

A top-to-S/SW brittle shear took place throughout the HHC (Figs. 6, 7) bound by a number of Y-planes that dip ∼ towards NE. The brittle shear is revealed in terms of inclined brittle planes (the P-planes) of various curvatures bound by parallel sets of shear planes (the Y-planes) with cm (Fig. 6a) up to ∼ a metre spacing (Fig. 6c). The termination of a number of P-planes across the Y-plane is a well-known feature (such as fig. 6.23a in Bahat et al. 2005). Sometimes, instead of a well-developed pair (Fig. 6a, c), only a single Y-plane is found (Fig. 6b). A single brittle plane may be weavy that locally define the Y-plane, and elsewhere the P-plane (Fig. 6b). Boudinaged quartz clasts may subsequently thrust giving rise

to sigmoid lenses (Fig. 6d). Along with distinct P-planes, the rock rarely resembles 'hard ash', which may be due to substantial shear heating (photographs with the author).

Step-overs or 'oversteps' of top-to-S/SW brittle shear cut the pre-existing top-to-S/SW brittle shear bound within NE dipping Y-planes (Fig. 7). The Y-planes of oversteps are undulatory and usually are sub-horizontal to gently dipping. At places, they converge and diverge to produce nearly symmetric lenses (Fig. 7c). These lenses alone are not indicative of shear sense. The Y-planes at places are sharp and devoid of any gouge (Fig. 7a, b). At other places, P-planes developed inside gouge zones (Fig. 7d).

Interestingly, an additional top-to-N/NE sense of brittle shear as backthrusts was documented from the HHC (Figs. 8, 9, 10) except its northern portion of Gangotri Granite. Backthrusts occur here as a zone, with lengths of individual thrusts up to several metres. The distances amongst these backthrusts are up to about half a metre. Their Y-planes dip moderate to steeply towards S/SW and bound sigmoid to nearly straight P-planes. The Y-planes may be restricted as a particular zone inside the rock (Fig. 8a). There are observations that only a set of P-planes developed devoid of any Y-planes (Fig. 8b, c). Both the Y-planes and the P-planes cut across the NE dipping main foliation (particularly Fig. 8c, d). The P-planes developed
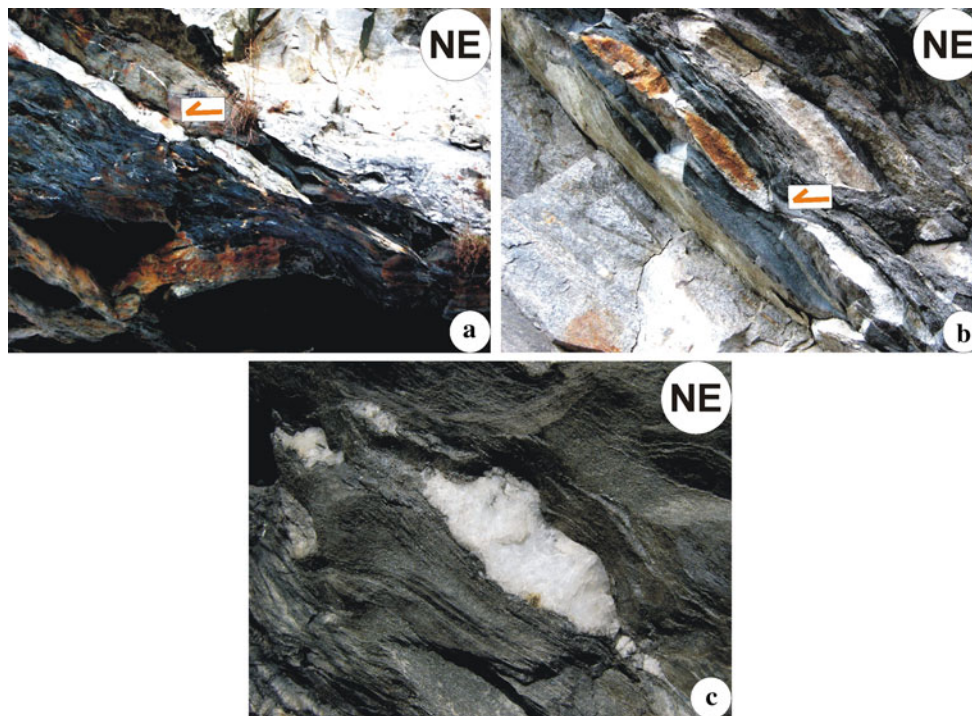
Fig. 5 Boudins of quartz veins from the HHC. Local brittle ductile shear (*orange half arrows*) in **a**, **b**; **a** photo widths: 26 cm. Location: 30°48′1.8″N, 78°37.0″E. **b** Photo width: 21 cm. Location: 30°48′1.8″N, 78°37.0″E. **c** Photo width: 12 cm. Location: 30°54′18.1″N; 78°40′44.5″E

at various extents—for example, few centimetre up to about few metres (Fig. 9b). Few of the P-planes are not so well developed (Fig. 10a). Individual P-planes curve sigmoidally inside brittle sheared sigmoid bulges (Fig. 10b). Shapes of bulges/lenses may not give any shear sense. Spacing between individual Y-planes may vary (Fig. 10c), Fore-thrusts (top-to-S/SW shear sense) and backthrusts (top-to-N/NE shear sense) sometimes constitute 'triangular zones'.

Brittle shear senses inside the Gangotri Granite are different and are less commonly developed than the remainder of the HHC. For example, the brittle shear is top-to-N/NE extensional (Fig. 11a), top-to-E compressional (Fig. 11b), top-to-S/SW extensional (Fig. 11c, d), top-to-N extensional (Fig. 12a), top-to-WSW compressional (Fig. 12b) and top-to-E compressional (Fig. 12c). These senses can be deciphered either in sub-vertical sections where the asymmetry of the P-planes is visible (Fig. 12a, c, d) or based on triangular peaks developed on the fault planes containing slickenlines (Fig. 11b). The Y-planes may or may not be developed in pairs (compare Fig. 12c with d) even for the same brittle shear sense. The spacing between the two adjacent P-planes changes along their length (Fig. 12a). The upper portion of the HHC, viz. the STDS, and most notably the vast exposure of the Gangotri Granite did not backthrust in a top-to-N/NE sense.

Discussions

Detachments

A structural summary of the Bhagirathi section of the HHC is presented schematically in Fig. 13. Since the demarcated deformation shear zones inside the HHC were only surface observations, their extent and geometries below the surface remains speculative. The basal detachment developed inside the HHC that partly overlaps the MCT-Zone corroborates similar findings from other sections such as from the Langtang section in Nepal (Takagi et al. 2003), Sutlej valley (Vannay et al. 2004; Mukherjee and Koyi 2010a) in the western Himalaya and the Mangde Chu river section in Bhutan (Jain et al. 2012). While Vannay et al. (2004), in their designated 'Karcham Normal Fault', did not deduce any activation timings, Takagi et al. (2003) deciphered Pliocene–Pleistocene Periods as the possible range of activation. From these limited information, Yin (2006) proposed that possibly the MCT acted as an extensional shear zone during the Cenozoic. This is despite the magnitude and consequence(s) of slip remained unknown. Other than these, Guillot (1999) reviewed several cases of MCT activity during the post-Miocene time. Presence of an extensional shear zone inside the HHC has been reported from the central and the eastern Himalaya (Godin et al. 2006's review). However, unlike those reported from the
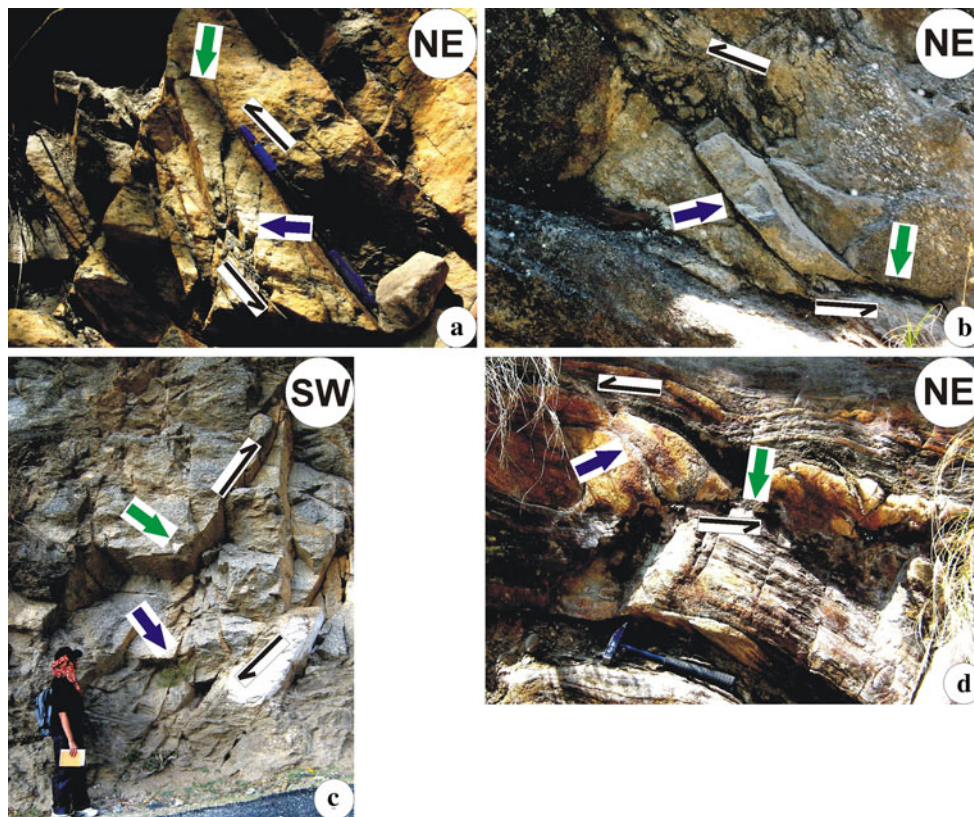
Fig. 6 Top-to-SW brittle sense of shear defined by P-planes (*blue full arrow*) and Y-planes (*green full arrow*). **b** A pair of P-planes are curved and sub-parallel. Photo width: 18 cm. Location: 30°45′23.2″N; 78°34′37.8″E. **d** A boudinaged clast of quartz developed P-planes. Location: 30°50′3.5′/N; 78°37′22.9″E

Nepalese Himalaya where it is a brittle extensional shear zone (Searle 1999a), the basal detachment in the Bhagirathi section is defined by a zone of top-to-N/NE ductile shear fabrics (Fig. 3). Presence of two ductile detachments from the Sutlej section was explained by Mukherjee and Koyi (2010a) as due to shifting mode of channel flow of the HHC (Fig. 14a). A shifting channel flow was also proposed by Hollister and Grujic (2006) who explained the out-of-sequence thrusting from the Bhutan Himalaya (Fig. 14b). In such shifting modes, one of the pulses of channel flow (extrusive pressure gradient plus shear at the boundaries) took place on the entire HHC. In the other pulse, channel flow (of the same meaning) was restricted at the southern sub-zone within the HHC. The northern boundary of this sub-zone is demarcated by the top of the basal detachment and the southern boundary the MCT_L. Mukherjee et al. (2012) demonstrated that simultaneous development of two detachments inside the HHC is kinematically implausible given the parallel or diverging-up geometry of the boundaries of the HHC. For converging-up boundaries as proposed by Webb et al. (2007), two detachments probably cannot develop simultaneously. Thus, despite the absence of timing of extensional shear of the basal detachment, channel flow in shifting mode might gave rise to the two

detachments. However, which detachment developed earlier remains unresolved. This is because although some estimate for the activation of the STDS by extensional ductile shear is already known (23–21 Ma: Searle et al. 1999; <21.9 Ma: Harrison et al. 1997, no movement of the Jhala Fault during ~21 Ma), that for the basal detachment is unavailable.

A number of geoscientific papers support channel flow of the HHC in the Garhwal Himalaya. The partially molten rock that Nelson et al. (1996) documented in southern Tibet at a mid-crustal depth continues presumably ~5 km below the MCT-zone (Israil et al. 2008; Ashish et al. 2009). Two phases of magmatism from the Bhagirathi section of the HHC at ~46 and ~20 Ma were interpreted as the pulses of channel flow (Jain et al. 2005).

Step-overs/oversteps

'Oversteps' (Ahlgren 2001), form lozenges (like fig. 13 of Fusseis et al. 2006) of a uniform asymmetry that gives the shear sense. Step-overs were described initially from strike slip fault zones (de Paola et al. 1996). Later, it seems to be common in other shear zones as well (e.g. Ponce et al. 2012). These authors explained the morphology of such lozenges
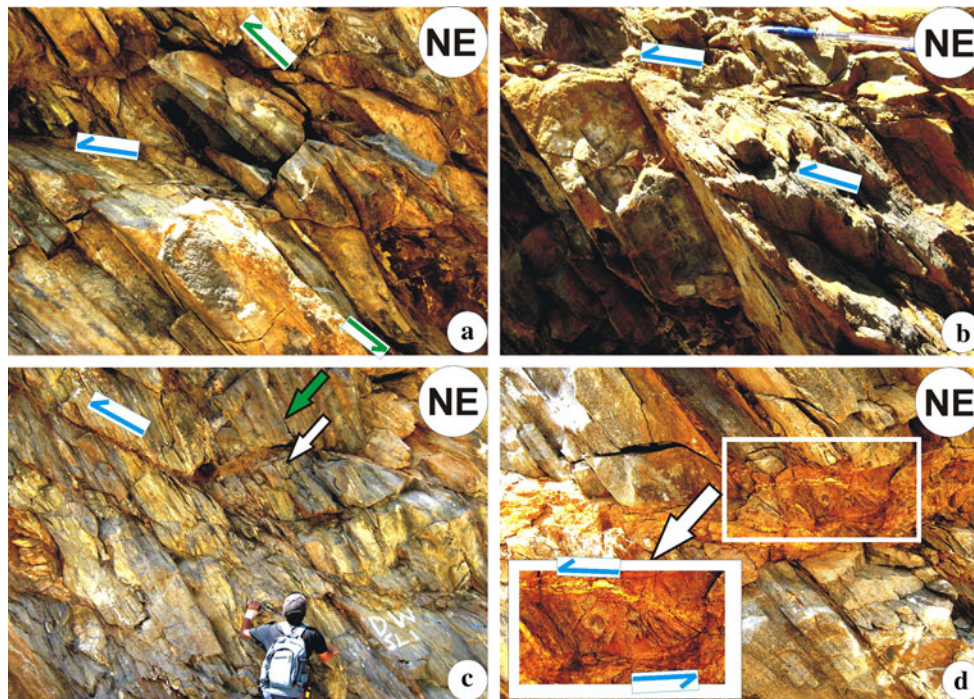
Fig. 7 **a–c** Step-overs shown by *blue half arrows*, developed for a top-to-S/SW brittle shear- shown by *green half arrow*. **c.** Intersecting Y-plane of step-over forms a lens (*white full arrow*). The NE dipping fracture plane is pointed by a *green arrow*. **d** The Y-plane of the step-over forms gouge where brittle shear planes and sense developed. Photo width: 14 cm. Location: 31°01′00″N; 78°42′34.9″E
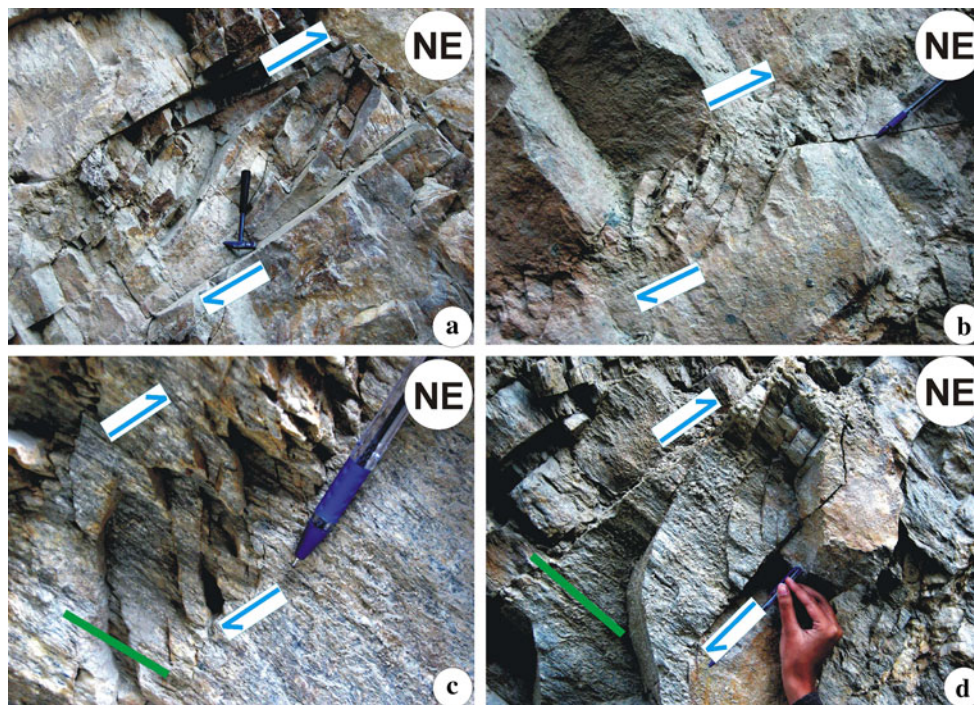

Fig. 8 Top-to-NE sense of brittle shear (*blue half arrows*) inside the HHC. Well-developed Y-planes in **a** and **d** but not in **b** and **c**. NE dipping main foliation (*green line*) is cut by the P-planes. Location: 31°51′50.6″N; 78°39′2.8″E
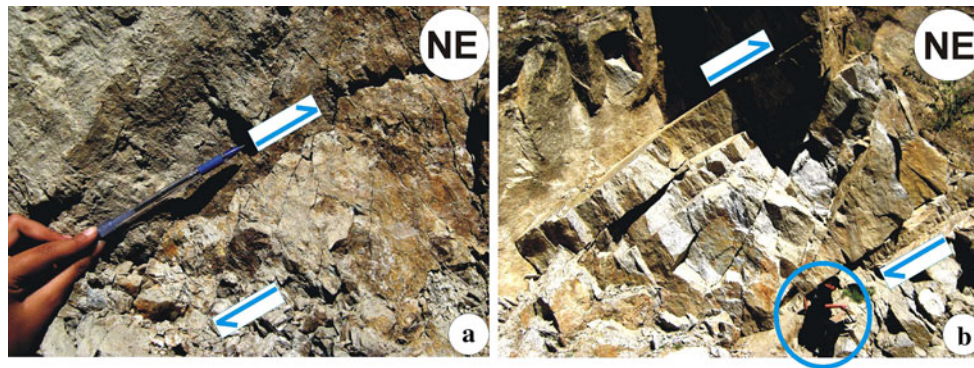
Fig. 9 Top-to-NE sense of brittle shear (*blue half arrows*) inside the HHC. **a**, **c** Indistinct Y-planes. **b** *blue ellipse*: a geologist as a marker. Locations: 31°51′37.7″N; 78°39′3.8″E
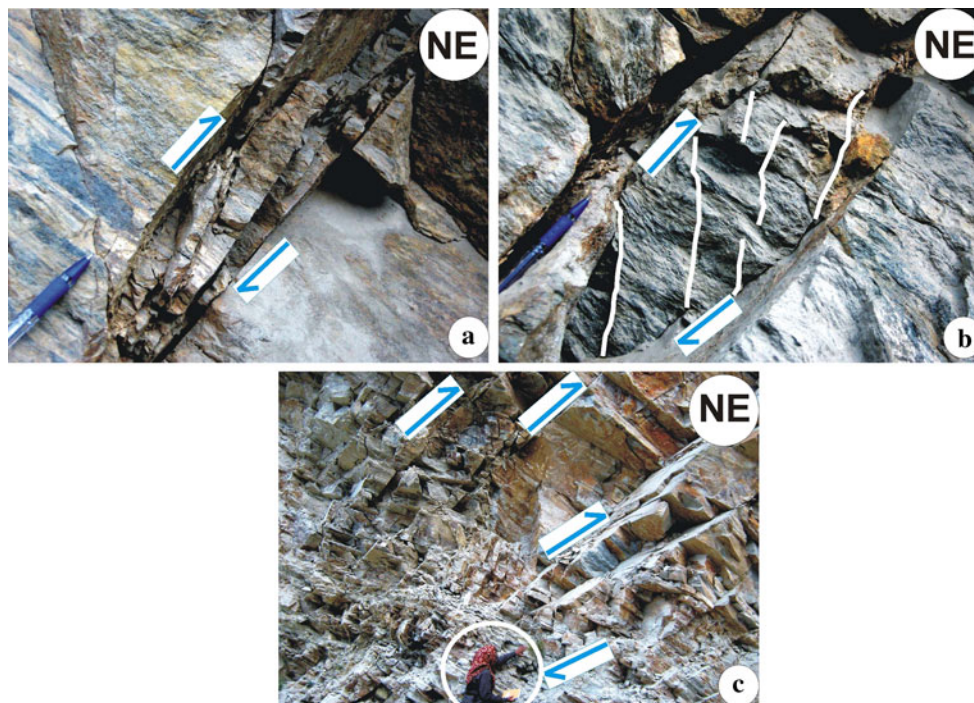

Fig. 10 Top-to-NE sense of brittle shear inside the HHC. That in **c** is of a much larger scale (*white circle*: a geologist as a marker). Location: 31°51′7.8″N; 78°38′22.3″E

from a shear zone in Cap de Creus area (eastern Pyrenees). They describe the lozenges, which are less deformed than the matrix, have no relation between their shapes to the strain and the deformation kinematics. Lozenges form due to intersection between the ductile primary (C) and the secondary shear planes (C′ and C″), but the detail mechanism is yet not clear (Ponce et al. 2010). The long axes of the lozenges make a low angle to the 'mean trend of the deformation zone' (i.e. the C-planes) at <30°. The lozenges were divided into four morphological categories: rhombic, lensoidal, rhomboidal and sigmoid (Ponce et al. 2012). In this study area, lensoidal and sigmoidal lenses are common. As in ductile shear zones (fig. 5 of Pereira and Silva 2004), the

step-overs in the HHC developed in the brittle regime due to intersection of the primary brittle shear Y-planes and local synthetic Riedel shear (Fig. 7c). The Y-planes are low-dipping and weavy. The networking of top-to-S/SW brittle shear zones possibly indicates deformation partitioning during this shear (Fusseis et al. 2006).

Backthrusts

Backthrusts were noted from various orogens in the Earth, mainly in collisional orogens including accretionary prisms. From the Himalaya in particular, backthrusts have been reported from the Siwalik and the Lesser Himalaya
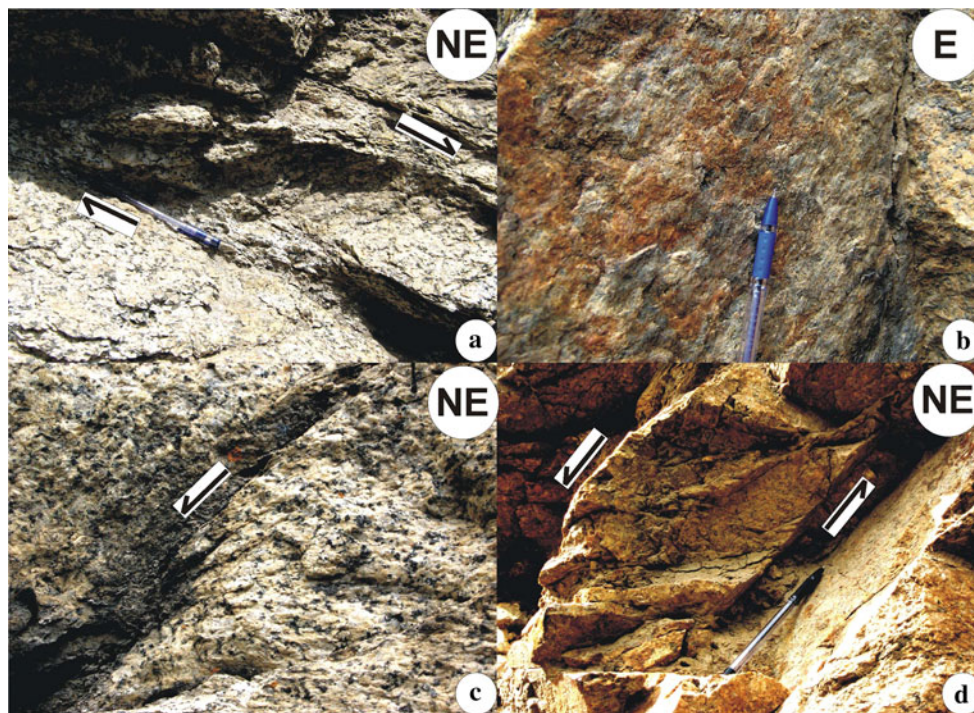
Fig. 11 Diverse shear senses documented from the Gangotri Granite. **a** Top-to-NE extensional, at 31°02′36.6″N, 78°50′31.2″E. **b** Slickenslides with triangular apices pointing up-dip. Top-to-E compressional, at 31°02′6.8″N, 78°51′32.1″E. **c** Top-to-SW extensional, at 31°02′6.8″N, 78°51′32.1″E. **d** Top-to-SW extensional, at 31°1′47.8″N; 78°52′6″E
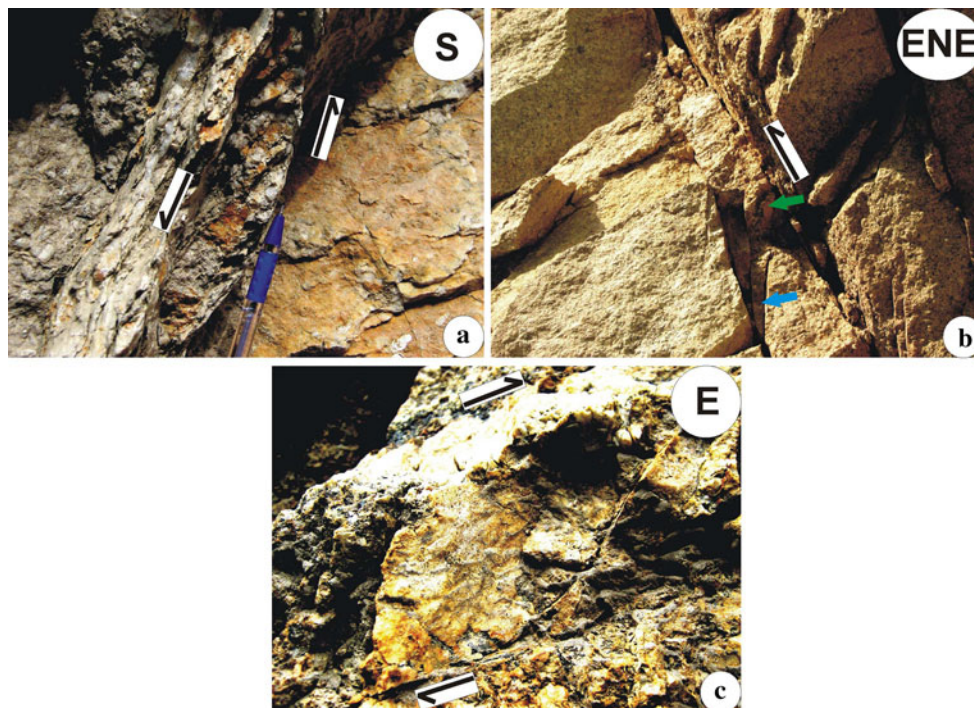

Fig. 12 Diverse shear senses documented from the Gangotri Granite. **a** Top-to-N extensional; at 31°01′27.7″N, 78°52′9.8″E. **b** Spacing between adjacent P-planes differ (at *green* and *blue full arrows*). Top-to-WSW compressional, at 31°01′27.7″N, 78°52′9.8″E. **c** Top-to-E compressional, at 31°01′24.8″N, 78°52′12.7″E

Fig. 13 The dominant structural geology of the HHC, Bhagirathi section, is summarized in a NE–SW cross-section. *HHC* Higher Himalayan Crystalline; MCT_L Main Central Thrust-Lower; *LH* Lesser Himalaya; MCT_U Main Central Thrust-Upper; *BD* Basal Detachment; *STDS* South Tibetan Detachment System; *TH* Tethyan Himalaya; *1* top-to-NW ductile compressional shear; *2* top-to-NE ductile extensional shear; *3* Boudins; *4* top-to-SW brittle compressional shear; *5* top-to-NE brittle compressional shear (backthrust); *6* top-to-SW brittle extensional shear; *7* top-to-N extensional brittle shear. The diagram is neither to scale nor angle
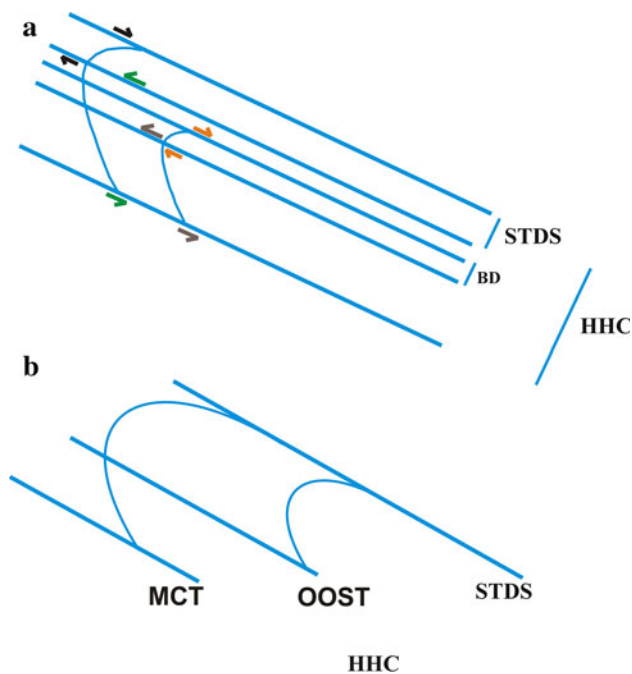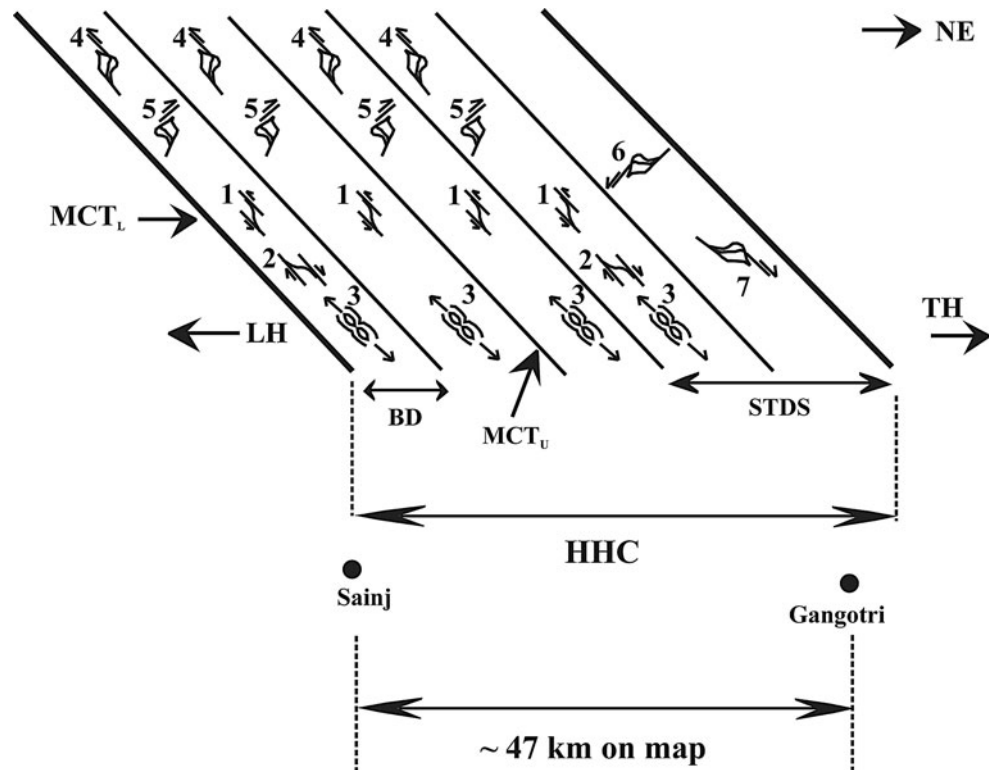

Fig. 14 Shifting channel flow model proposed from the HHC. **a** Across the vertices of the parabolic flow profiles, ductile shear sense reverses. *Lines* parallel to the boundaries of the HHC passing through the vertex define the *lower* boundary of the detachment. Drawn from fig. 17 of Mukherjee and Koyi (2010a). *Half arrows* represent the ductile shear senses of sub-zones that they bound. **b** One of the flow pulses is bound by the OOST. Drawn from fig. 5 of Hollister and Grujic (2006). *HHC* Higher Himalayan Crystalline; *STDS* South Tibetan Detachment System; *BD* Basal Detachment; *OOST* Out-of-sequence thrust; *MCT* Main Central Thrust

(Chalaron et al. 1995; Mugnier et al. 1998; Powers et al. 1998; Mugnier et al. 1999, Mukhopadhyay and Mishra 2005; Yin 2006 and references therein; Guha et al. 2007; Thakur et al. 2007; Malik et al. 2010; review by Kumarahara and Jayangondaperumal 2013). The 'Great Counter Thrust' (GCT/South Kailash Thrust System/Renbu-Zedang Thrust/Himalayan backthrust/Main Zanskar Backthrust)—that demarcates the boundary between the Tethyan sediments in S and the Asian plate in N—is a backthrust with N/NE vergence and dominantly a southward movement and folding of the hanging wall block (Heim and Gansser 1939; Yin et al. 1999). The GCT thrust system consists of five or more individual thrusts (Murphy and Yin 2003) that affect only the top portion of the crust, slipped at a rate of ~ 7 mm year^{-1} during 30–23 Ma (Harrison et al. 2000) and has a two-stage tectonic evolution (Yin et al. 1999) with a displacement of ≥ 12 km (Quidelleur et al. 1997). The GCT acted coevally with the Main Central Thrust (MCT) and the STDS at south and the backthrusts of the south central Tibet at $\sim$ mid-Miocene Period (Hébert et al. 2012). Based on U–Th/He dating, Tripathi (2011) obtained the timing of GCT between 19 and 7 Ma. This posed doubt whether GCT, MCT and STDS acted coevally and whether GCT can be considered as a single thrust system. It extends regionally from the western up to the eastern Himalaya. The Great Counter Thrust shows some strike slip evidences as well (Zhang et al. 2011). The thrust has been deciphered in sub-surface based on seismic anisotropic studies

Fig. 15 Subduction of the Indian plate below Tibet took place as by wedging between it and the ductile lower crust of the Eurasian plate. Reproduced from fig. 10.11 of Fielding (2000). Geographical directions (N/NE, S/SW) are added
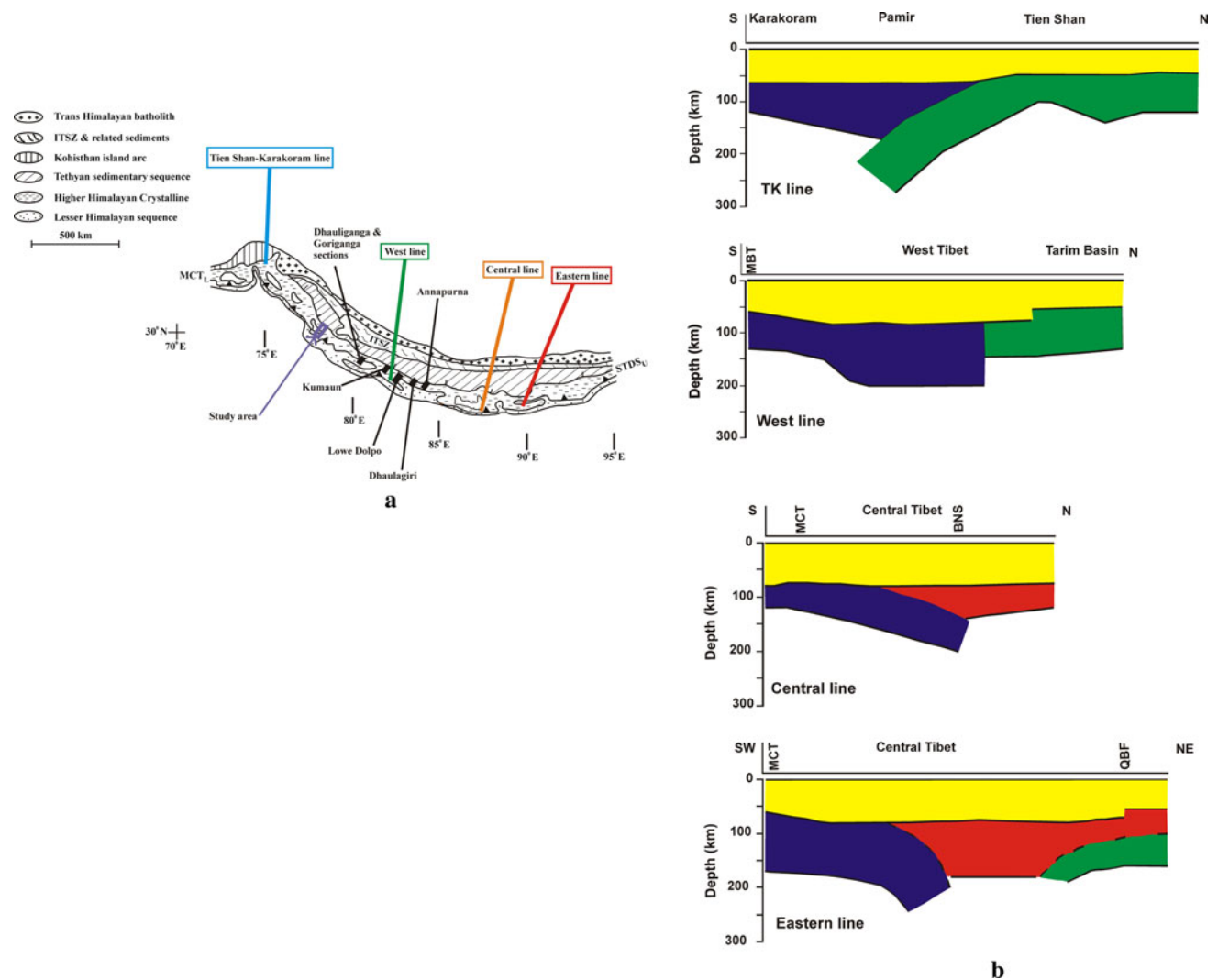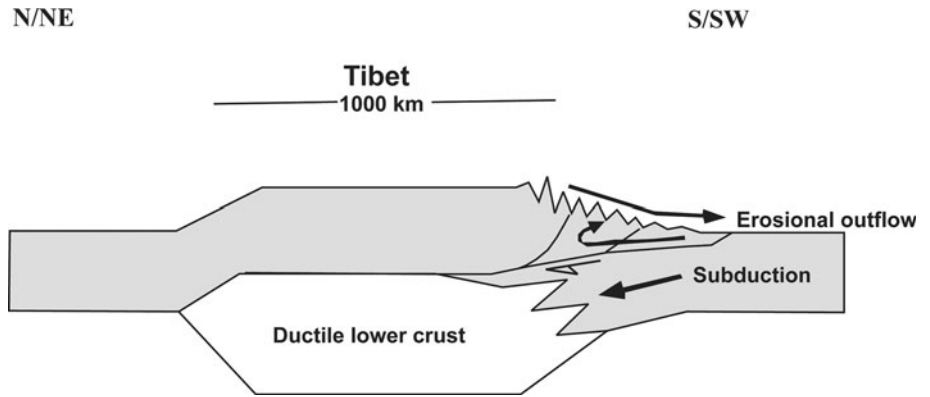

Fig. 16 Geophysical studies undertaken across the Himalayan trend, taken from fig. 1 of Zhao et al. (2010), is drawn on the Himalaya map reproduced from fig. 1 of .Godin et al. (2006). **b** Crustal section along those lines reproduced from fig. 4 of Zhao et al. (2010). *Green* Asian mantle lithosphere; *red* crush zone; *yellow* crust; *blue* Indian mantle lithosphere. *MBT* Main Boundary Thrust; *MCT* Main Central Thrust; *BNS* Bangong-Nujiang Suture; *QBF* Quaidam Basin Fault

(Sherrington et al. 2004). In SE Tibet, the Great Counter Thrust oriented magnetic lineations a SSW trend (Antolín et al. 2011). Since the link between this thrust and the STDS has remained doubtful (Yin 2006), the existing tectonic models of the Higher Himalaya do not refer it. No backthrusts were reported from the Higher Himalaya from

field before the present work. Thus, the observed back-thrusts in this section is not regionally extensive along the Himalayan trend. Notice that very recently, however, the STDS has been proposed to be a backthrust (e.g. He et al. 2012; Kellett and Grujic 2012; Webb and He 2012).

The tendency of the viscous channel flow alone that initiates from south Tibet is to produce folds and ductile shear zones with a NE vergence inside the STDS and a SW vergence within the remainder of the HHC. Thus, back-thrusting of the HHC cannot be explained to push on the brittle rocks by ductile extrusion from bottom. Instead, the critical taper model could be useful to explain them. Backthrusting becomes dominant near the bottom of the taper zones of the wedge, and they become equally frequent as the fore-thrusts for a low taper angle (Bilotti and Shaw 2005). Backthrusts develop the taper condition within the wedge (McQuarrie and DeCelles 2001).

Backthrusts may develop when low-frictional material passes from a flat into a ramp (Butler 1987; Maillot and Leroy 2003; Nieuwland et al. 2010). In the present case, a low friction between the channel boundaries and the extruding material is expected since the HHC during extrusion was in a partially molten state. Partial melting was achieved by shear heating: (1) over the MCT ramp (Harrison et al. 1997); (2) below south Tibet possibly due to crustal thickening and overpressure (review by Harris 2007); and (3) around the central zone of the HHC (Mukherjee 2012c). Alternately, the melt could have come from (4) the fluids released from the underlying Lesser Himalaya (Guo and Wilson 2011); and/or (5) melting of the HHC rocks in situ (e.g. the Haimanta-Cheka Formation in Nepal: Searle et al. 2010). Given these different sources, the resultant softening of the HHC is expected to be non-uniform yet significant.

Backthrusting can develop in collisional settings either due to reversal of polarity of subduction, due to an inter-ference between varied isostatic uplift and horizontal compression in collisional regimes (review in Kroehler et al. 2011; Moores and Twiss 1995), or by deformation of several rock layers under compression (Albanese and Sulli 2012). Interestingly, Fielding (2000) presented in his crustal section that the Indian plate subducted below the Eurasian plate not just as a slab (discussed later) but pen-etrated the ductile lower crust of the Eurasian plate as a wedge (Fig. 15). Our textbook idea that the Indian plate subducted as a coherent unit below the Eurasian plate from the Late Jurassic, and the oceanic portion of the Eurasian plate subducted during Late Triassic to Earle Jurassic (e.g. fig. 10.15 in Keary et al.2009) got fine tuned with upcoming many seismic tomographic studies (review by Kumar 2012; fig. 4 of Guillot and Replumaz 2013; Replumaz et al. 2013). Zeng et al. (2007) deciphered from seismic anomalies documented from a section between

Lhasa to Golmud (Tibet) that there could be several northward and southward subductions in the India-Eurasia collisional regime. Chen et al. (2010) deciphered that the Indian mantle lithosphere got detached from its crustal counterpart and moved significantly northward below the Eurasian plate. In other words, the Indian crust and the Indian lithospheric mantle did not act as a single unit (Replumaz et al. 2010). Liang et al. (2012) interpreted that the upper mantle beneath the Tibetan plateau is possibly subducting southward below the Indian plate. Flow of mantle towards south has been predicted to corroborate this from mathematical models (Zahirovic et al. 2012). Tomographic studies have deciphered shallow but signifi-cant southward subduction of the Eurasian plate in Pamir region (Negredo et al. 2007; also see Mechie et al. 2012; Schneider et al. 2012), which happened at a slower rate than that of the Indian plate (see Vignon et al. 2011), and probably initiated before ∼21 Ma (Lukens et al. 2012). Robinson et al. (2012) deciphered southward subduction of the Asian oceanic crust during early Jurassic Period. This was subsequently supported by gravity studies by Tiwari et al. (2010). Even a flip in the subduction direction of the Indian plate from north to south has been reported (Kou-lakov and Sobolev 2006). Kumar et al. (2006) deciphered by seismic studies from Lhasa (Tibet) that the Eurasian plate there subducted up to ∼175 km depth southward at a moderate angle. The Eurasian plate could have moved below the Indian plate in a sub-horizontal manner (Yue et al. 2012). Zhao et al. (2010) presented a more detailed scenario that the Asian mantle lithosphere remains sub-horizontal below Pamir and Karakoram and dips southward to reach ∼250 km depth, whereas in the eastern Himalaya, along the 'eastern line', this subduction is more restricted (nearly the same transect what Kumar et al. 2006 worked earlier); no subduction has been deciphered in the central section of the orogen through the 'central line'(Fig. 16; also see Kind et al. 2010 for a similar conclusion). A similar west to east fall in southward advance of the Eur-asian mantle was also deciphered by Li et al. (2008). It thus appears that the Eurasian plate was not merely static withstanding compression of the Indian plate, but the for-mer also actively pushed and moved southward. The zone in between the subducted mantle slabs of the Indian and the Eurasian plates could either be a 'crush zone' of rocks (Zhao et al. 2010) or a hot mantle diapir (Zhang et al. 2012). This supports Zhao et al.'s (2011) postulation that the lithospheric architecture in the India-Eurasia subduc-tion zone is indeed complex.

The present observation of numerous backthrusts doc-umented in the field within the entire HHC from the Bhagirathi section locates nearly equidistant from the Tien Shan-Karakoram line and the West line along which the deep seismic images were presented by Zhao et al. (2010).

The 'West line' of Zhao et al. (2010) is in close proximity with Lower Dolpo, Annapurna, Dhaulagiri (Nepal), and Dhauliganga and Goriganga sections (India) (shown in Fig. 16a). Therefore, further structural fieldworks in these sections might reveal backthrusts inside the HHC. The likelihood of getting backthrusts much away from this area seems unlikely except the Pamir region where southward subduction of both the Indian and the Eurasian plates have been deciphered (Koulakov and Sobolev 2006; Negredo et al. 2007). In several recent seismic studies, ~400 km subduction of the Indian plate has been deciphered. This could be due to a corner flow of the Indian asthenosphere stronger than that of the Eurasian asthenopshere (fig. 5 of Fu et al. 2008; fig. 9 of Yue et al. 2012).

Brittle shear

One of the theories of brittle shear is that the shear plane Y-forms first. This is followed by the P-planes at an angle to the Y-planes. The P-planes (~ 'fault arrays'), usually sigmoid, originates from the Y-planes and migrate towards the nearest other Y-plane (Fusseis et al. 2006; see Fig. 17). In the HHC, this is evidenced by (1) the dominant NE dipping fractures ubiquitously developed inside the HHC (excepting the Gangotri Granite) and the Y-planes for the top-to-S/SW brittle shear have nearly same attitude and (2) sometimes P-planes of half-sigmoid shapes emanate from the NE dipping Y-planes. This also possibly indicates that the top-to-S/SW brittle shear acted along many of the pre-existing NE dipping fracture planes. These fractures locally acted as the Y-planes and developed brittle P-planes.

A number of brittle shear senses documented from the Gangotri Granite cannot be explained simply in terms of backthrusting towards the hinterland side (i.e. towards N/NE direction). Assuming that the HHC once attained a critical taper condition, at least the top-to-S/SW extensional brittle shear can readily be explained in terms of wedge tectonics of the HHC. Matching the push of the model wedge materials towards SW same as the direction of extrusion of the HHC, one can explain top-to-S/SW extensional shear. Further, backthrusts and out-of-sequence
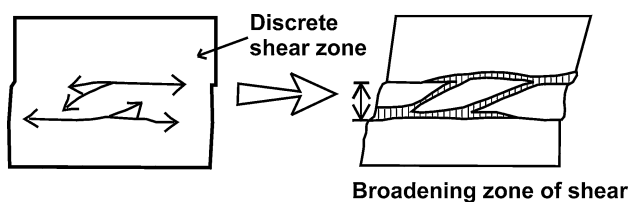

Fig. 17 Evolution of brittle shear zones as presented by Tchalenko (1970) and summarized by Handy et al. (2007). After branching out from the Y-planes that migrate along their lengths, the P-planes tend to join sigmoidally with the adjacent Y-plane

thrusts are the manifestations of wedge mechanics (Platt 1986). The observed backthrusts throughout the HHC support a wedge mechanism/critical taper model of extrusion which might have acted for the HHC.

Conclusions

In addition to a top-to-S/SW shear, two sub-zones (STDS, basal detachment) of top-to-N/NE shear are demarcated inside the Bhagirathi river section of the Higher Himalayan Crystalline (HHC). The upper boundary of the STDS also demarcates the top of the HHC. The lower margin of the former lies around the middle of the HHC. The extensional shear zone 'Jhala Fault' falls inside the STDS. The basal detachment occurs within the southern portion of the Main Central Thrust-Zone (MCTZ). Besides a top-to-S/SW brittle shear (fore thrusting), a series of top-to-N/NE backthrusts characterize the HHC except its northern portion occupies by the Gangotri Granite. The S/SW shear is characterized by step-overs that indicate strain localization. The Gangotri Granite displays a number of other extensional and compressional brittle shear senses. Two ductile sub-zones inside the HHC might be produced by shifting channel flow of the HHC. Pure shear leading selectively to the detachment inside in HHC (here the 'basal detachment') was considered to be tectonically implausible by Mukherjee and Koyi (2010a) from the Sutlej section of the Himalaya. Backthrusting from the HHC was hitherto not reported from any section of the Higher Himalaya. These backthrusts cannot be correlated with any out-of-sequence thrusting since such deformation has not been documented from the present study area in the Bhagirathi section. Significant subduction of the Eurasian plate below the Indian plate in the Garhwal Himalaya could develop these backthrusts. It appears that the top-to-S/SW brittle shear developed along Y-planes that previously acted merely as NE dipping fractures. The critical taper model can explain at least the top-to-S/SW extensional shear inside the Gangotri Granite. It thus appears that both channel flow and critical taper exhumation mechanisms acted inside the HHC. It might be possible that the hot partially molten mid-crustal material after being extruded to the brittle regime was under wedge tectonics. This is in accordance with the recent numerical models by Beaumont and Jamieson (2010), geochronologic findings by Chambers et al. (2011), Larson et al. (2011), Long et al. (2012) and thermobarometric works by Corrie et al. (2012) and Larson et al. (2013).

Caldwell et al. (2012) based on geophysical evidences postulated the presence of a ramp and flat geometry of the HHC in the Garhwal region (also reviewed by Rai and Ramesh 2012; Singh et al. 2012; see Gahalaut and Arora 2012). Change in Moho depth within the Higher Himalaya as deciphered from gravity studies from an eastern (Tiwari

et al. 2010) and a western Himalayan section (Chamoli et al. 2011) could also be an indicator of ramp and flat geometry. Such a thrust geometry can favour a critical taper situation.

References

Ahlgren SG (2001) The nucleation and evolution of Riedel shear zones as deformation bands in porous sandstones. J Struct Geol 23:1203–1214

Albanese C, Sulli A (2012) Backthrusts and passive roof duplexes in fold-and-thrust belts—the case of Central-Western Sicily based on seismic reflection data. Tectonophysics 514–517:180–198

Antolín B, Appel E, Montomoli C et al (2011) Kinematic evolution of the eastern Tethyan Himalaya: constraints from magnetic fabric and structural properties of the Triassic flysch in SE Tibet. In: Poblet J, Lisle RJ (eds) Kinematic evolution of and structural styles of fold-and-thrust belts. Geol Soc Lond Spec Publ 349:99–121

Argles TW, Edwards MA (2002) First evidence of high-grade, Himalayan age synconvergent extension recognized within the western syntaxis—Nanga Parbat, Pakistan. J Struct Geol 24:1327–2344

Ashish PadhiA, Rai SS et al (2009) Seismological evidence for shallow crustal melt beneath the Garhwal High Himalaya, India: implications for the Himalayan channel flow. Geophys J Int 177:1111–1120

Bahat D, Rabinovitch A, Frid V (2005) Tensile fracturing in rocks. Springer, Berlin

Beaumont C, Jamieson RA (2010) Himalayan–Tibetan Orogeny: channel flow versus (critical) wedge models, a false dichotomy? In: Leech ML et al (eds) Proceedings for the 25th Himalaya–Karakoram–Tibet workshop: U.S. Geological Survey, Open-File Report

Beaumont C, Jamieson RA, Nguyen MH et al (2001) Himalayan tectonics explained by extrusion of a low-viscosity crustal channel coupled to focused surface denudation. Nature 414:738–742

Berthé D, Choukroune P, Jegouzo P (1979) Orthogneiss, mylonite and non-coaxial deformation of granite: the example of the south Armorican shear zone. J Struct Geol 1:31–42

Bilotti F, Shaw JH (2005) Deep water Niger Delta fold and thrust belt modeled as a critical taper wedge: the influence of elevated basal fluid pressure on structural styles. AAPG Bull 89:1475–1491

Brown RL, Gibson HD (2006) An argument for channel flow in the southern Canadian Cordillera and comparison with Himalayan tectonics. In: Law RD, Searle MP, Godin L (eds) Channel flow, ductile extrusion and exhumation in continental collision zones. Geol Soc Lond Spec Publ 268:541–557

Butler RWH (1987) Thrust sequences. J Geol Soc Lond 144:619–634

Caldwell WB, Klemperer SL, Lawrence JF et al (2012) Characterizing the Main Himalayan Thrust in the Garhwal Himalaya, India with receiver function CCP stacking. Earth Planet Sci Lett (in review)

Carosi R, Lombardo B, Molli G et al (1998) The South Tibetan detachment system in the Rongbuk valley, Everest region. Deformation features and geological implications. J Asian Earth Sci 16:299–311

Carosi R, Montomoli C, Iaccarino S et al (2013) Tectono-metamorphic discontinuities in the Greater Himalayan Sequence and their role in the exhumation of crystalline units. Geophysical Research Abstracts, vol 15, European Geosciences Union General Assembly, Vienna, Austria (submitted)

Catlos EJ, Harrison TM, Manning CE et al (2002) Records of the evolution of the Himalayan orogen from in situ Th–Pb ion microprobe dating of monazite: Eastern Nepal and western Garhwal. J Asian Earth Sci 20:459–479

Catlos EJ, Dubey CS, Marston RA et al (2007) Geochronologic constraints across the Main Central Thrust shear zone, Bhagirathi river (NW India): implications for Himalayan tectonics. In: Cloos M, Carlson WD, Gilbert MC et al (eds) Convergent margin terranes and associated regions: a tribute to W.G. Ernst. Geol Soc Am Spec Pap 135–151

Chalaron E, Mugnier JL, Mascle G (1995) Control on thrust tectonics in the Himalayan foothills: a view from a numerical model. Tectonophysics 248:139–163

Chambers J, Parrish R, Argles T et al (2011) A short duration pulse of ductile normal shear on the outer South Tibetan detachment in Bhutan: alternating channel flow and critical taper mechanics of the eastern Himalaya. Tectonics 30:TC2005

Chamoli A, Pandey AK, Dimri VP et al (2011) Crustal Configuration of the Northwest Himalaya based on modeling of gravity data. Pure Appl Geophys 168:827–844

Chen W-P, Martin M, Tseng T-L et al (2010) Shear-wave birefringence and current configuration of converging lithosphere under Tibet. Earth Planet Sci Lett 295:297–304

Corrie SL, Kohn MJ, McQuarrie N et al (2012) Flattening the Bhutan Himalaya. Earth Planet Sci Lett 349–350:67–74

Davis GH, Reynolds SJ (1996) Structural geology of rocks and regions, 2nd edn. Wiley, New York

de Paola N, Holdsworth RE, Clollettini C et al (1996) The structural evolution of dilational stepovers in regional transtensional zones. In: Cunningham WD, Mann P (eds) Tectonics of strike-slip restraining and releasing bends. Geol Soc Lond Spec Publ 290:433–445

Edwards MA, Kidd WSF, Li J et al (1996) Multi-stage development of the southern Tibet detachment system near Khula Kangri: new data from Gonto La. Tectonophysics 260:1–19

Fielding EJ (2000) Morphotectonic evolution of the Himalaya and Tibetan plateau. In: Summerfield MA (ed) Geomorphology and global tectonics. Wiley, New York, pp 201–222

Fu YV, Chen YJ, Li A et al (2008) Indian mantle corner flow at southern Tibet revealed by shear wave splitting measurements. Geophys Res Lett 35:L02308

Fusseis F, Handy MR, Schrank C (2006) Networking of shear zones at the brittle to viscous transition (Cap de Creus, NE Spain). J Struct Geol 28:1228–1243

Gahalaut VK, Arora BR (2012) Seismicity along the Himalayan Arc due to structural heterogeneities in the underthrusting Indian plate and overriding Himalayan wedge. Episodes 35:493–500

Gehrels G, Kapp P, DeCelles P et al (2011) Detrital zircon geochronology of pre-tertiary strata in the Tibetan–Himalayan orogens. Tectonics 30:TC5016

Godin L, Grujic D, Law RD et al (2006) Channel flow, extrusion and exhumation in continental collision zones: an introduction. In:

Law RD, Searle MP (eds) Channel flow, extrusion and exhumation in continental collision zones. Geol Soc Lond Spec Publ 268:1–23

Goscombe B, Gray D, Hand M (2006) Crustal architecture of the Himalayan metamorphic front in eastern Himalaya. Gond Res 10:232–255

Grasemann B, Fritz H, Vannay JC (1999) Quantitative kinematic flow analysis from the Main Central Thrust Zone (NW-Himalaya, India): implications for a decelerating strain path and extrusion of orogenic wedges. J Struct Geol 21:837–853

Guha D, Bardhan S, Basir SR et al (2007) Imprints of Himalayan thrust tectonics on the Quaternary piedmont sediments of the Neora–Jaldhaka Valley, Darjeeling–Sikkim Sub-Himalayas, India. J Asian Earth Sci 30:464–473

Guillot S (1999) An overview of the metamorphic evolution in Central Nepal. J Asian Earth Sci 17:713–725

Guillot S, Replumaz A (2013) Importance of continental subductions for the growth of the Tibetan plateau. Bull de la Société Géol de France (in press)

Guo Z, Wilson M (2011) The Himalayan leucogranites: constraints on the nature of their crustal source region and geodynamic setting. Gond Res 22:360–376

Handy MR, Hirth G, Bürgmann R (2007) Continental fault structure and rheology from the frictional-to-viscous transition downward. In: Handy MR, Hirth G, Hovius N (eds) Chapter 6: Tectonic faults: agents of change on a dynamic earth. The MIT Press, Cambridge, pp 139–181

Harris NBW (2007) Channel flow and the Himalayan–Tibetan orogen: a critical review. J Geol Soc Lond 164:511–523

Harrison TM, Lovera OM, Grove M (1997) New insights into the origin of two contrasting Himalayan granite belts. Geology 25:899–902

Harrison TM, Yin A, Grove M et al (2000) The Zedong Window: a record of superposed tertiary convergence in southeastern Tibet. J Geophys Res 105:19211–19230

He D, Webb AAG, Larson KL et al (2012) New findings from crystalline rocks of the frontal klippen, Nepal Himalaya demonstrate mountain-building via underplating. Abstract in 27th Himalaya–Karakoram–Tibet workshop (HKT). J Nepal Geol Soc 45:40

Hébert R, Bezard R, Guilmette C et al (2012) The Indus–Yarlung Zangbo ophiolites from Nanga Parbat to Namche Barwa syntaxes, southern Tibet: first synthesis of petrology, geochemistry, and geochronology with incidences on geodynamic reconstructions of Neo-Tethys. Gond Res 22:377–397

Heim A, Gansser A (1939) Central Himalaya, geological observations of the Swiss expeditions 1936. Memoires de la Société Helvetiques des Sciences Naturelles 73:1–245

Hollister LS, Grujic D (2006) Pulsed channel flow in Bhutan. In: Law RD, Searle MP, Godin L (eds) Channel flow, ductile extrusion and exhumation in continental collision zones. Geol Soc Lond Spec Publ 268:415–423

Israil M, Tyagi DK, Gupta PK et al (2008) Magnetotelluric investigations for imaging electrical structure of Garhwal Himalayan corridor, Uttarakhand, India. J Earth Syst Sci 117:189–200

Jain AK, Singh S, Manickavasagam RM (2002) Himalayan collisional tectonics. Gondwana Research Group Memoir No. 7. Field Science, Hashimoto

Jain AK, Manickavasagam RM, Singh S et al (2005) Himalayan collision zone: new perspectives—its tectonic evolution in a combined ductile shear zone and channel flow model. Himal Geol 26:1–18

Jain AK, Singh S, Sushmita et al (2012) Structurally controlled melt formation and accumulation: evidence for channel flow in the Himalaya. Abstract in 27th Himalaya–Karakoram–Tibet workshop (HKT). J Nepal Geol Soc 45:2

Johnson MRW, Harley SL (2012) Orogenesis: the making of mountains. Cambridge University Press, Cambridge, pp 1–325

Keary P, Klepeis KA, Vine FJ (2009) Global tectonics, 3rd edn. Wiley-Blackwell, Hoboken

Kellett DA, Grujic D (2012) New insight into the South Tibetan detachment system: not a single progressive deformation. Tectonics 31:TC2007

Khannal S, Robinson DM (2012) Upper crustal shortening and forward modeling of the Himalayan thrust belt along the Budhi-Gandaki River, central Nepal. Int J Earth Sci (submitted)

Kind R, Zhao J, Yuan X et al (2010) The structure of the colliding plates beneath Tibet. European Geosciences Union General Assembly, Abstract, 2–7 May 2010, Vienna, Austria, p 9422

Kirby E, Whipple KX (2012) Expression of active tectonics in erosional landscapes. J Struct Geol 44:54–75

Koulakov I, Sobolev SV (2006) A tomographic image of Indian lithosphere break-off beneath the Pamir–Hindukush region. Geophys J Int 164:425–440

Kroehler ME, Mann P, Escalona A et al (2011) Late Cretaceous–Miocene diachronous onset of back thrusting along the South Caribbean deformed belt and its importance for understanding processes of arc collision and crustal growth. Tectonics 30:TC6003

Kumar P (2012) Seismic structure beneath Tibet from receiver functions: a review. Deep Cont Stud India Newsl 22:8–11

Kumar P, Yuan X, Kind R et al (2006) Imaging the colliding Indian and Asian lithospheric plates beneath Tibet. J Geophys Res 111:B06308

Kumarahara Y, Jayangondaperumal R (2013) Paleoseismic evidence of a surface rupture along the northwestern Himalayan Frontal Thrust (HFT). Geomorphology 180–181:47–56

Iaccarino S, Montomoli C, Carosi R et al (2013) Linking microstructures, petrology and in situ U-(Th)-Pb geochronology to constrain P-T-t-D evolution of the Greater Himalyan Sequences in Western Nepal (Central Himalaya). Geophysical Research Abstracts, vol 15, European Geosciences Union General Assembly, Vienna, Austria (submitted)

Larson KP, Godin L (2009) Kinematics of the Himalayan metamorphic slab, Dhaulagiri Himal: implications for the structural framework of the central Nepalese Himalaya. J Geol Soc Lond 166:25–43

Larson KP, Godin L, Price RA (2010) Relationships between displacement and distortion in orogens: linking the Himalayan foreland and hinterland in central Nepal. Geol Soc Am Bull 122:1116–1134

Larson KP, Cottle JM, Godin L (2011) Petrochronologic record of metamorphism and melting in the upper Greater Himalayan sequence, Manaslu–Himal Chuli Himalaya, west-central Nepal. Lithosphere 3:379–392

Larson KP, Gervais F, Kellett DA (2013) Tectonic Insight from P-T-t paths, upper Tama Koshi region, Nepal. J Nepal Geol Soc 45:79

Law RD, Searle MP, Simpson RL (2004) Strain, deformation temperatures and vorticity of flow at the top of the Greater Himalayan slab, Everest massif. Tibet J Geol Soc Lond 161:305–320

Li C, van der Hilst RD, Meltzer AS (2008) Subduction of the Indian lithosphere beneath the Tibetan Plateau and Burma. Earth Planet Sci Lett 274:157–168

Liang X, Sandvol E, Chen YJ et al (2012) A complex Tibetan upper mantle: a fragmented Indian slab and no south-verging subduction of Eurasian lithosphere. Earth Planet Sci Lett 333–334:101–111

Linero PR (2008) Analyses of vertical thermochronologic profiles in the High Crystalline Himalaya with allowance for advection of heat: interactions among exhumation, climate, and tectonics. University of Colorado, Denver, pp 27–30

Lombardo B, Pertusati P, Borghi S (1993) Geology and tectonomagmatic evolution of the eastern Himalaya along the Chomolungma–Makalu transect. In: Treloar PL, Searle MP (eds) Himalayan tectonics. Geol Soc Lond Spec Publ 74:341–356

Long SP, McQuairrie N, Tobgay T et al (2012) Variable shortening rates in the eastern Himalayan thrust belt, Bhutan: insights from multiple thermochronologic and geochronologic datasets tied to kinematic reconstructions. Tectonics 31:TC5004

Lukens CE, Carrapa B, Singer BS et al (2012) Miocene exhumation of the Pamir revealed by detrital geothermochronology of Tajik rivers. Tectonics 31:TC2014

Maeder X, Passchier CW, Koehn D (2009) Modelling of segment structures: boudins, bone-boudins, mullions and related single- and multiphase deformation features. J Struct Geol 31:817–830

Maillot B, Leroy YM (2003) Optimal dip based on dissipation of back thrusts and hinges in fold-and-thrust belts. J Geophys Res 108:2320

Malavieille J, Chemenda A, Larroque C (1998) Evolutionary model for Alpine Corsica: mechanism for ophiolite emplacement and exhumation of high-pressure rocks. Terra Nova 10:317–322

Malik J, Shah AA, Sahoo AK et al (2010) Active fault, fault growth and segment linkage along the Janauri anticline (frontal foreland fold), NW Himalaya, India. Tectonphysics 483:327–343

McQuarrie N, DeCelles P (2001) Geometry and structural evolution of the central Andean backthrust belt, Bolivia. Tectonics 20:669–692

Mechie J, Yuan X, Schurr B et al (2012) Crustal and uppermost mantle velocity structure along a profile across the Pamir and southern Tien Shan as derived from project TIPAGE wide-angle seismic data. Geophys J Int 188:385–407

Metcalfe RP (1993) Pressure, temperature and time constraints on metamorphism across the Main Central Thrust zone and High Himalayan slab in the Garhwal Himalaya. In: Treloar PJ, Searle MP (eds) Himalayan tectonics. Geol Soc Spec Publ 74:485–509

Mitra G, Bhattacharyya K, Mukul M (2010) The lesser Himalayan duplex in Sikkim: implications for variations in Himalayan shortening. J Geol Soc Ind 75:289–301

Moores EM, Twiss RJ (1995) Tectonics. W.H. Freeman, New York, pp 1–415

Morley CK (1988) Out-of-sequence thrusts. Tectonics 7:539–561

Mugnier JL, Delcaillau B, Huyghe P et al (1998) The break-back thrust splay of the Main Dun Thrust (Himalayas of western Nepal): evidence of an intermediate displacement scale between earthquake slip and finite geometry of thrust systems. J Struct Geol 20:857–864

Mugnier JL, Leturmy P, Mascle G et al (1999) The Siwaliks of western Nepal I. Geometry and kinematics. J Asian Earth Sci 17:629–642

Mukherjee S (2011) Mineral fish: their morphological classification, usefulness as shear sense indicators and genesis. Int J Earth Sci 100:1303–1314

Mukherjee S (2012a) Viscous dissipation pattern in incompressible Newtonian simple shear zones—analytical model & application in the Higher Himalaya. Int J Earth Sci (submitted)

Mukherjee S (2012b) Channel flow extrusion model to constrain dynamic viscosity and Prandtl number of the Higher Himalayan Shear Zone. Int J Earth Sci (in press)

Mukherjee S (2012c) Sequel of Mukherjee. Int J Earth Sci (submitted)

Mukherjee S (2012d) Simple shear is not so simple! Kinematics and shear senses in Newtonian viscous simple shear zones. Geol Mag 149:819–826

Mukherjee S, Bandyopadhyay A (2011) Structural geology of the Bhagirathi section of the Higher Himalayan Shear Zone with special reference to back-thrusting. International conference on Indian monsoon and Himalayan geodynamics, 2–5 Nov 2011. Wadia Institute of Himalayan Geology, Dehradun, India

Mukherjee S, Koyi HA (2010a) Higher Himalayan Shear Zone, Sutlej section: structural geology and extrusion mechanism by various combinations of simple shear, pure shear and channel flow in shifting modes. Int J Earth Sci 99:1267–1303

Mukherjee S, Koyi HA (2010b) Higher Himalayan Shear Zone, Zanskar Indian Himalaya—microstructural studies & extrusion mechanism by a combination of simple shear & channel flow. Int J Earth Sci 99:1083–1110

Mukherjee S, Mukherjee B (2012) Meeting report: session: "geodynamics of collision type orogenic belts and plateaus and its response to climate and erosional processes—Himalaya, Pamir, 1638 Central Asia and Tibet" TS 4.5: European Geosciences Union 2012, Vienna, Austria. J Geol Soc Ind (submitted)

Mukherjee S, Mulchrone K (2012) Estimating the viscosity and Prandtl number of the Tso Morari crystalline gneiss dome, Indian western Himalaya. Int J Earth Sci 101:1929–1947

Mukherjee S, Koyi HA, Talbot CJ (2012) Implications of channel flow analogue models for extrusion of the Higher Himalayan Shear Zone with special reference to the out-of sequence thrusting. Int J Earth Sci 101:253–272

Mukhopadhyay DK, Mishra P (2005) A balanced cross section across the Himalayan frontal fold-thrust belt, Subathu area, Himachal Pradesh, India: thrust sequence, structural evolution and shortening. J Asian Earth Sci 25:735–746

Murphy MA, Yin A (2003) Structural evolution and sequence of thrusting in the Tethyan fold-thrust belt and Indus–Yalu suture zone, southwest Tibet. GSA Bull 115:21–34

Negredo AM, Replumaz A, Villaseñor A et al (2007) Modeling the evolution of continental subduction processes in the Pamir–Hindu Kush region. Earth Planet Sci Lett 259:212–225

Nelson KD, Zhao W, Brown LD et al (1996) Partially molten middle crust beneath Southern Tibet: synthesis of project INDEPTH results. Science 274:1684–1688

Nieuwland DA, Leutscher JH, Gast J (2010) Wedge equilibrium in fold-and-thrust belts: prediction of out-of-sequence thrusting based on sandbox experiments and natural examples. Geol en Mijn 79:81–91

Panian J, Pilant W (1990) A possible explanation for foreland thrust propagation. J Geophys Res 95:8607–8615

Passchier CW, Trouw RAJ (2005) Microtectonics, 2nd edn. Springer, Berlin

Patel RC, Singh S, Asokan A et al (1993) Extensional tectonics in the Himalayan orogen, Zanskar, NW India. In: Treloar PJ, Searle MP (eds) Himalayan Tectonics, vol 74. Geological Society of London, Special Publication, pp 445–459

Pereira MF, Silva JB (2004) Development of local orthorhombic fabrics within a simple-shear dominated sinistral transpression zone: the Arronches sheared gneisses (Iberian Massif, Portugal). In: Alsop GI, Holdsworth RE, McCaffrey et al (eds) Flow processes in faults and shear zones, vol 224. Geological Society of London, Special Publication, pp 215–227

Platt JP (1986) Dynamics of orogenic wedges and the uplift of high-pressure metamorphic rocks. Geol Soc Am Bull 97:1037–1053

Ponce C, Carreras J, Druguet E (2010) Development of "lozenges" in anastomosing shear zone networks in foliated rocks. Geogaceta 48:207–210

Ponce C, Druguet E, Carreras J (2012) Development of shear zone-related lozenges in foliated rocks. J Struct Geol (in press)

Powers PM, Lillie RJ, Yeats RS (1998) Structure and shortening of the Kangra and Dehra Dun reentrants, Sub-Himalaya, India. Geol Soc Am Bull 110:1010–1027

Quidelleur X, Grove M, Lovera OM et al (1997) Thermal evolution and slip history of the Renbu-Zedong thrust, southeastern Tibet. J Geophys Res 102:2659–2679

Rai S, Ramesh DS (2012) Seismic imaging of the Indian continental lithosphere. In: Singhvi AK, Banerjee DM (eds) Glimpse of geoscience research in India: Indian report to IUGS: 2008–2012. Proc Indian Nat Sci Acad 78:353–359

Replumaz A, Negredo AM, Guillot S et al (2010) Multiple episodes of continental subduction during India/Asia convergence: insight

from seismic tomography and tectonic reconstruction. Tectonophysics 483:125–134

Replumaz A, Guillot S, Villaseñor A et al (2013) Amount of Asian lithospheric mantle subducted during the India/Asia collision. Gond Res (in press)

Rivers T (2009) The Grenville province as a large hot long-duration collisional orogen—insights from the spatial and thermal evolution of its orogenic fronts. In: Murphy JB, Keppie JD, Hynes AJ (eds) Ancient orogens and modern analogues. Geol Soc Lond Spec Publ 327:405–444

Robinson AC, Ducea M, Lapen TJ (2012) Detrital zircon and isotopic constraints on the crustal architecture and tectonic evolution of the northeastern Pamir. Tectonics 31:TC2016

Roy AB, Valdiya KS (1988) Tectonometamorphic evolution of the Great Himalayan Thrust Sheets in Garhwal Region, Kumayaun Himalaya. J Geol Soc Ind 32:106–124

Sachan HK, Sharma R, Sahai A et al (2001) Fluid events and exhumation history of the Main Central Thrust Zone, Garhwal Himalaya. J Asian Earth Sci 19:207–221

Sachan HK, Kohn MJ, Saxena A et al (2010) The Malari leucogranite, Garhwal Himalaya, northern India: chemistry, age and tectonic implications. Geol Soc Am Bull 122:1865–1876

Sapkota J, Sanislav IV (2012) Preservation of deep Himalayan PT conditions that formed during multiple events in garnet cores: mylonitization produces erroneous results for rims. Tectonophysics (in press)

Scaillet B, Pêcher A, Rochette P et al (1995) The Gangotri granite (Garhwal Himalaya): laccolithic emplacement in an extending collisional belt. J Geophys Res 100(B1):585–607

Schmalholz SM, Maeder X (2012) Pinch-and-swell structure and shear zones in viscoplastic layers. J Struct Geol 37:75–88

Schneider FM, Yuan X, Sippl C et al (2012) Evidence for southward subduction beneath the eastern Pamir constrained by teleseismic converted seismic waves. European Geosciences Union General Assembly, Austria

Searle MP (1999) Extensional and compressional faults in the Everest–Lhotse massif, Khumbu Himalaya, Nepal. J Geol Soc Lond 156:227–240

Searle MP, Metcalfe RP, Rex AJ et al (1993) Field relations, petrogenesis and emplacement of the Bhagirathi leucogra-nite, Garhwal Himalaya. In: Treloar PJ, Searle MP (eds) Himalayan tectonics. Geol Soc Lond Spec Publ 429–444

Searle MP, Noble SR, Hurford AJ et al (1999) Age of crustal melting, emplacement and exhumation history of the Shivling leucogra-nite, Garhwal Himalaya. Geol Mag 136:513–525

Searle MP, Cottle JM, Streule MJ et al (2010) Crustal melt granites and migmatites along the Himalaya: melt source, segregation, transport and granite emplacement mechanisms. Earth Env Sci Trans R Soc Edinb 100:219–233

Sherrington HF, Zandt G, Frederiksen A (2004) Crustal fabric in the Tibetan plateau based on waveform inversions for seismic anisotropy parameters. J Geophys Res 109:B02312

Singh K, Thakur VC (2001) Microstructures and strain variation across the footwall of the Main Central Thrust Zone, Garhwal Himalaya, India. J Asian Earth Sci 19:17–29

Singh S, Mukherjee PK, Jain AK (2003) Source characterization and possible emplacement mechanism of collision-related Gangotri Leucogranite alonh Bhagirathi Valley, NW-Himalaya. In: Singh S (ed) Granitoids of the Himalayan collisional belt. J Virtual Explor 11:Paper 06

Singh P, Patel RC, Lal N (2012) Plio-Plistocene in-sequence thrust propagation along the Main Central Thrust zone (Kumaon–Garhwal Himalaya, India): new thermochronological data. Tectonophysics 574–575:193–203

Sorkhabi RB, Stump E, Foland KA et al (1996) Fissiontrack and $^{40}Ar/^{39}Ar$ evidence for episodic denudation of the Gangotri

granites in the Garhwal Higher Himalaya, India. Tectonophysics 260:187–199

Sorkhabi RB, Stump E, Foland K, Jain AK (1999) Tectonic and cooling history of the Garhwal Higher Himalaya (Bhagirathi Valley): constraints from thermochronological data. In: Jain AK, Manickavasagam RM (eds) Geodynamics of the NW Himalaya, vol 6. Gondwana Research, Group Memoir, pp 217–235

Srivastava HB, Tripathi NR (2007) Geometrical analysis of meso-scopic shear zones in the crystalline rocks of MCT zone of Garhwal Higher Himalaya. J Asian Earth Sci 30:599–612

Srivastava HB, Sahai A, Lal SN (2000) Strain and crystallographic fabric in mesoscopic ductile Shear Zones of Garhwal Himalaya. Gond Res 3:395–405

St-Onge MR, Searle MP, Wodicka N (2006) Trans-Hudson Orogen of North America and Himalaya-Karakoram-tibet Orogen of Asia: structural and thermal characteristics of the lower and upper plates. Tectonics 25:TC4006

Streule MJ, Strachan RA, Searle MP et al (2010) Comparing Tibet–Himalayan and Caladonian crustal architecture, evolution and mountain building processes. In: Law RD, Butler RWH, Holdsworth RE et al (eds) Continental tectonics and mountain building: the legacy of peach and hone. Geol Soc Lond Spec Publ 335:207–232

Takagi H, Arita K, Sawaguchi T et al (2003) Kinematic history of the Main Central Thrust zone in the Langtang area, Nepal. Tectonophysics 366:151–163

Tchalenko JS (1970) Similarities between Shear Zones of different magnitudes. Geol Soc Am Bull 81:1625–1640

Thakur VC, Pande AK, Suresh N (2007) Late Quaternary–Holocene evolution of Dun structure and the Himalayan Frontal Fault zone of the Garhwal Sub-Himalaya, NW India. J Asian Earth Sci 29:305–319

Tiwari VM, Singh B, Arora K et al (2010) The potential of satellite gravity and gravity gradiometry in deciphering structural setting of the Himalayan collision zone. Curr Sci 99:1795–1800

Tripathi A (2011) Exploring the history of India–Eurasia collision and subsequent deformation in the Indus Basin, NW Indian Himalaya. PhD thesis, Arizona State University, pp 146–150

Tripathi NR, Srivastava HB (2005) Mesoscopic ductile shear zones from the Main Central Thrust zone of Bhagirathi Valley, Garhwal Higher Himalaya. Curr Sci 88:815–821

Tripathi N, Srivastava HB, Mamtani M (2009) Evaluation of a regional strain gradient in mylonitic quartzites from the footwall of the Main Central Thrust Zone (Garhwal Himalaya, India): inferences from finite strain and AMS analyses. J Asian Earth Sci 34:26–37

Twiss RJ, Moores EM (2007) Structural Geology, 2nd edn. W.H. Freeman, New York

van Hinsbergen DJJ, Lippert PC, Dupont-Nivet G et al (2012) Greater India Basin hypothesis and a two-stage Cenozoic collision between India and Asia. PNAS 109:7659–7664

Vannay J-C, Grasemann B, Rahn M et al (2004) Miocene to Holocene exhumation of metamorphic crustal wedges in the NW Himalaya: evidence for tectonic extrusion coupled to fluvial erosion. Tectonics 23:TC1014

Vignon V, Replumaz A, Guillot S et al (2011) Geometry, timing and consequences of subduction processes in the Pamir and Hindu Kush regions. Geophysical Research Abstracts, vol 13, European Geosciences Union 2011-8944

Wang K (2007) Elastic and viscoelastic models of crustal deformation in subduction earthquake cycles. In: Dixon TH, Moore JC (eds) The seismogenic zone of subduction thrust faults. Columbia University Press, New York, pp 540–575

Webb AA, He D (2012) The South Tibetan Detachment is a backthrust: new evidence from studies along the length of the Himalayan orogen. Abstract in the 27th Himalaya–Karakoram–Tibet workshop (HKT). J Nepal Geol Soc 45:1

Webb AAG, Yin A, Harrison TM et al (2007) The leading edge of the Greater Himalayan crystallines revealed in the NW Indian Himalaya: implications for the evolution of the Himalayan Orogen. Geology 35:955–958

Yakymchuk C, Godin L (2012) Coupled role of deformation and metamorphism in the construction of inverted metamorphic sequences: an example from far-northwest Nepal. J Meta Geol 30:513–535

Yang J, Xu Z, Robinson PL et al (2011) HP-UHP metamorphic belts in the Eastern Tethyan Orogenic System in China. In: Dobrzhinetskaya LF, Faryad SW, Wallis S et al (eds) Ultrahigh-pressure metamorphism: 25 years after the discovery of coesite and diamond. Part IV: ultrahigh-pressure metamorphic belts and protolith history of eclogite and garnet peridotite. Elsevier, Amsterdam, pp 459–499

Yin A (2006) Cenozoic tectonic evolution of the Himalayan orogen as constrained by along-strike variation of structural geometry, extrusion history, and foreland sedimentation. Earth Sci Rev 76:1–131

Yin A, Harrison TM, Murphy MA et al (1999) Tertiary deformation history of southeastern and southwestern Tibet during the Indo-Asian collision. GSA Bull 111:1644–1664

Yue H, Chen J, Sandvol E et al (2012) Lithospheric and upper mantle structure of the northeast Tibetan Plateau. J Geophys Res 117:B05307

Zahirovic S, Müller D, Seton M et al (2012) Insights on the kinematics of the India–Eurasia collision from global geodynamic models. Geochem Geophys Geosys 13:Q04W11

Zeng R-S, Wu Q-J, Ding Z-F et al (2007) Indian Eurasian collision vs. ocean–continent collision. Acta Seismol Sin 20:1–10

Zhang ZM, Zhao GC, Santosh M et al (2010) Two stages of granulite facies metamorphism in the eastern Himalayan syntaxis, south Tibet: petrology, zircon geochronology and implications for the subduction of Neo-Tethys and the Indian continent beneath Asia. J Meta Geol 28:719–733

Zhang R, Murphy MA, Lapen TJ et al (2011) Late Eocene crustal thickening followed by Early-Late Oligocene extension along the India–Asia suture zone: evidence for cyclicity in the Himalayan orogen. Geosphere 7:1249–1268

Zhang H, Zhao D, Zhao J et al (2012) Convergence of the Indian and Eurasian plates under eastern Tibet revealed by seismic tomography. Geochem Geophys Geosys 13:Q06W14

Zhao J, Yuan X, Liu H et al (2010) The boundary between the Indian and Asian tectonic plates below Tibet. Proc Natl Acad Sci 107:11229–11233

Zhao W, Kumar P, Mechie J et al (2011) Tibetan plate overriding the Asian plate in central and northern Tibet. Nat Geosci 4:870–873